Chemical Geology 581 (2021) 120396

Contents lists available at ScienceDirect

Chemical Geology

journal homepage: www.elsevier.com/locate/chemgeo

Invited Research Article

Calcium isotope cosmochemistry

Maria C. Valdes [a,b,c,*], Katherine R. Bermingham [d,e], Shichun Huang [f], Justin I. Simon [g]

[a] Robert A. Pritzker Center for Meteoritics and Polar Studies, Negaunee Integrative Research Center, The Field Museum of Natural History, Chicago, IL, USA
[b] Department of Geophysical Sciences, The University of Chicago, Chicago, IL, USA
[c] Department of Earth Sciences, University of Cambridge, Cambridge, UK
[d] Department of Earth and Planetary Science, Rutgers University, Piscataway, NJ, USA
[e] Department of Geology, University of Maryland, College Park, MD, USA
[f] Department of Geoscience, University of Nevada, Las Vegas, NV, USA
[g] Center for Isotope Cosmochemistry and Geochronology, Astromaterials Research and Exploration Science, NASA Johnson Space Center, Houston, TX, USA

ARTICLE INFO

Editor: Don Porcelli

Keywords:
Calcium isotopes
Cosmochemistry
Meteorites
CAIs

ABSTRACT

The past decade has seen significant advancements in analytical capabilities and with it a marked increase in the use of Ca isotopes to advance our understanding of the Solar System's and Earth's evolution. Here, mass-dependent and non-mass-dependent Ca isotopic variations in bulk meteorites and chondrite components are discussed. This contribution also examines how Ca isotopes record nebular processes, including evaporation/condensation and mixing of chemically and isotopically distinct reservoirs in the protoplanetary disk. The applicability of non-mass-dependent Ca isotopic variations to tracing the nature and timing of stellar mass contributions to the parental molecular cloud is discussed. This includes the constraints Ca isotopic data provide on the nature of and the relationships between planetary building blocks. This contribution also explores the effects of parent body-based and terrestrial secondary processes, and variable sampling of isotopically heterogeneous Ca-rich components, on bulk meteorite compositions. Using the data reviewed here, this contribution attempts to reconcile the chemical and isotopic Ca data from bulk meteorites and meteorite components to address a major goal in planetary science, the development of a comprehensive model of the chemical and isotopic evolution of the Solar nebula into our planetary system.

1. Introduction

Understanding how a habitable planet formed requires an understanding of how its host planetary system and star evolved. The study of major elements and their isotopes, such as Ca, provides key constrains on the chemical evolution of the Solar System. The generalities of the process are understood, but much of the detail is yet to be revealed.

The Solar System originated from a portion of a parental molecular cloud which was composed of dust and gas that had accumulated from earlier generation stars. This includes dust that was added to the interstellar medium at least ~3 ± 2 Ga prior to the start of the Solar System (Heck et al., 2020). The cause of the separation between the protonebula and the main molecular cloud mass is debated (for a review, see Montmerle et al., 2006). It may have been caused by shockwaves from a neighboring supernova (Cameron and Truran, 1977; Boss, 1995) or sufficient weakening of the magnetic field support following ambipolar diffusion (Shu et al., 1987). This fragment formed a rotating disk (generally referred to as a protoplanetary disk) nested in the molecular cloud. At the center of the protoplanetary disk, the "proto-sun" began hydrogen fusion when sufficiently high temperature and pressure were reached. Subsequently, planets and their satellites grew out of the protoplanetary disk via accretion, a process that describes the coalescence of μm-sized solid particles into cm-sized pebbles, km-sized planetesimals, and finally the planets (for reviews, see Johansen and Lambrechts, 2017; Simon et al., 2018). Some of the material that did not accrete to the planets or their satellites remains in the Solar System as asteroids, where the majority of this mass is stored in the main asteroid belt (equivalent to ~4% of the Moon's mass) and lies between Mars and Jupiter. Some parent bodies in the asteroid belt are sampled by Earth in the form of meteorites. As remnants of the protoplanetary disk, meteorites can be used to constrain the chemical (e.g., elemental abundances) and isotopic building blocks of the Solar System and planets.

* Corresponding author at: Robert A. Pritzker Center for Meteoritics and Polar Studies, Negaunee Integrative Research Center, The Field Museum of Natural History, Chicago, USA.
E-mail address: mvaldes@fieldmuseum.org (M.C. Valdes).

https://doi.org/10.1016/j.chemgeo.2021.120396
Received 18 June 2019; Received in revised form 4 June 2021; Accepted 8 June 2021
Available online 15 June 2021

Meteorites are broadly classified into two groups: chondrites, which originate from unmelted (undifferentiated) parent bodies, and achondrites, which originate from melted (differentiated) parent bodies. Both groups provide important chemical and isotopic constraints on Solar System evolution. For example, through the comparison of element abundances in unmelted meteorites to the Sun's photosphere, it was concluded that CI chondrites provide the closest chemical match to the non-volatile[1] composition of the Solar nebula (Anders, 1971). Element abundances in meteorites have since been used to infer element fractionation due to nebular processing and parent-body igneous processes (e.g., Nittler et al., 2004). In combination with planetary observations, these and other chemical data obtained from meteorites indicate a relatively volatile depleted inner Solar System *vs.* a volatile enriched outer Solar System. Here, the inner and outer Solar System refers to inboard or outboard of Jupiter, respectively (following Warren, 2011).

Chondrites preserve discrete meteorite components that formed in the disk prior to the accretion of the parent body. The meteorite components were likely also sampled by achondrite parent bodies to varying degrees; however, differentiation mixed these components into the bulk composition of the body such that they are no longer visible. There are several types of refractory inclusions, chondrules, dark fragments, and dark inclusions found in chondrites. Here, these materials are collectively referred to as "chondrite components" and the constraints their Ca isotopic compositions provide on early Solar System evolution are discussed in Section 3. Calcium-aluminum-rich inclusions (CAIs) are one type of refractory inclusion which are among the first aggregates that formed from disk material. These refractory inclusions have an average condensation age of 4567.30 ± 0.16 Ga (Connelly et al., 2012) and in most cosmochemical studies this age defines "time zero" (t_0) and the start of the Solar System. The primary mineralogy of these inclusions is enriched in refractory elements (e.g., Ca, Al, and Ti) as oxides or silicates, which are among the first phases predicted to condense from a cooling gas of Solar composition (Grossman, 1972; Yoneda and Grossman, 1995; Petaev and Wood, 1998). As indicated by their complex mineralogy, CAIs experienced multiple heating and cooling events prior to incorporation into larger bodies (e.g., Petaev and Jacobsen, 2009). The coexistence of refractory inclusions and volatile elements (e.g., C, N, O) in some carbonaceous chondrites indicates large temperature gradients in the disk and mixing between different regions during the formation of some parent bodies.

Despite the different environments and thermal/chemical processing that occurred in the disk, a record of presolar dust is retained in meteorites (e.g., Lewis et al., 1987; Zinner et al., 1987; Dauphas et al., 2010; Mendybaev et al., 2002; Simon et al., 2019). Presolar grains, a type of presolar dust, formed in stellar outflows or ejecta and remained intact throughout their journey into the Solar System where they were preserved in meteorites (Lodders and Amari, 2005). Because presolar grains contain isotopes in relative abundances reflective of the stellar environment in which they formed, these grains have very different (vary on the ‰- to %-scale) compositions compared to material that formed from the protoplanetary disk (e.g., Burbidge et al., 1957; Cameron, 1957; Clayton et al., 1973; Lewis et al., 1987; Bernatowicz et al., 1987; Zinner et al., 1987; Amari et al., 1990; Zinner, 2014). Although only unmelted meteorites preserve these grains such that they can be isolated by chemical treatment, presolar dust was inherited by both melted and unmelted meteorites (Zinner, 2014). It is generally considered that presolar grains were heterogeneously distributed in the protoplanetary disk, where some grains may have been introduced to the Solar nebula after its initial accretion. The heterogeneous distribution of presolar material is indicated by the existence of variable non-mass-dependent isotopic compositions (so-called nucleosynthetic isotopic variations) in bulk meteorites and their components (see review by Qin and Carlson, 2016). By studying non-mass-dependent isotopic compositions in meteorites and their components, the stellar events that contributed material to the Solar System and their distribution in the protoplanetary disk can be identified.

This review synthesizes Ca isotopic variations in bulk meteorites[2] and their components with the constraints these data provide on the early stages of Solar System evolution. The focus is on how mass-dependent and non-mass-dependent Ca isotope effects provide information about the compositions of cosmochemical building blocks, thermal processing in the disk, and parent body alteration. It concludes with a summary of outstanding questions in cosmochemistry and the future avenues of research Ca isotopes present.

1.1. The role of Ca in cosmochemistry

Calcium is one of the most refractory elements in the Solar System (T_c = 1659 K; Lodders, 2020). Consequently, some Ca condensed into CAIs and other early formed meteorite components, thereby preserving chemical and isotopic information about the early disk. As Ca is a major component in asteroids (e.g., ~1–8 wt% in HEDs; Mittlefehldt, 2014) and terrestrial planets (2.52 wt% in bulk silicate Earth; McDonough and Sun, 1995), it can also be used to investigate parent body compositions, differentiation (Huang et al., 2010), and parent body alteration (Zolensky and McSween, 1988).

The utility of the Ca isotope system stems from the high number of stable Ca isotopes and the mass range they cover, the existence of a short-lived radioactive Ca isotope, and the diversity of nucleosynthetic pathways that produce Ca isotopes. Calcium comprises twenty-four isotopes, six of which (^{40}[3], 42, 43, 44, 46, and ^{48}[4]) are considered to be stable isotopes (Amos et al., 2011). The 20% range between the lightest and heaviest stable Ca isotopes is more than any element except for H and He (Clayton, 2004), which makes Ca isotopes a sensitive tool for recording mass-dependent isotopic fractionation. Cosmochemical Ca isotope studies exploit these features to track processes that generate Ca mass-dependent isotope fractionation, including nebular condensation and evaporation, parent body differentiation, and aqueous alteration.

Non-mass-dependent Ca isotopic compositions preserve information about the stellar sources that contributed material to the Solar nebula and how these were distributed in the disk (e.g., Dauphas et al., 2014a). The dominant nucleosynthetic pathways for Ca are listed in Table 1 and for detailed review of Ca isotope nucleosynthetic pathways and stellar sources see Burbidge et al. (1957), Meyer et al. (1996), and Wanajo et al. (2013). Also of cosmochemical relevance is the short-lived radioactive system ^{41}Ca–^{41}K (^{41}Ca $t_{1/2}$ = 103 ka), where ^{41}Ca forms via neutron capture on ^{40}Ca. The first definitive evidence for live ^{41}Ca in early Solar System came from correlating ^{41}K/^{39}K ratios with Ca/K in Efremovka (CV3) CAIs (Srinivasan et al., 1994, 1996), and subsequent studies of hibonites from Murchison (CM2) and Allende (CV3) (Sahijpal et al., 1998, 2000). Newer data on the same and additional CAIs (from NWA 3118 and Vigarano, both CV3) indicate that the early Solar System ^{41}Ca/^{40}Ca was lower than indicated in earlier works (Liu et al., 2012; Liu, 2017). Cosmic ray exposure ages can be calculated for meteorites and lunar soils using this short-lived radioactive system (Bogard et al., 1995; Nishiizumi et al., 1997).

[1] Refractory elements have 50% condensation temperatures (T_c) above 1335 K, moderately volatiles between 1335 and 665 K, volatile elements below 665 K, and highly volatile elements below 371 K. Condensation temperatures refers to the equilibrium condensation appearance temperature of an element into a compound (solid phase) from a Solar composition gas at 10^{-4} bar total pressure (Lodders, 2003).

[2] Bulk meteorite refers to a homogenized sample of the entire meteorite, as opposed to a sample of distinct meteorite components.

[3] ^{40}Ca abundances can be affected by the β-decay of ^{40}K (^{40}K $t_{1/2}$ = 1.25 Ga).

[4] ^{48}Ca is radioactive with a $t_{1/2}$ of 4.3 × 10^{19} years; however, its long half-life permits it to be considered a stable isotope.

Table 1
Stable Ca isotopes, their natural abundances, and nucleosynthetic pathways of production.

Isotope	Natural abundance	Nucleosynthesis
^{40}Ca	96.941	O and Si-burning
^{41}Ca[a]	–	Neutron capture on ^{40}Ca
^{42}Ca	0.647	O and Si-burning
^{43}Ca	0.135	O and Si-burning
^{44}Ca	2.086	Decay product of ^{44}Ti[b], produced during O and Si-burning
^{46}Ca	0.004	*s*-process
^{48}Ca[c]	0.187	Neutron-rich processes: Type Ia or e^- capture SN of AGB

[a] ^{41}Ca ($t_{1/2}$ = 103 ka).
[b] ^{44}Ti ($t_{1/2}$ = 60 a).
[c] ^{48}Ca is radioactive ($t_{1/2} = 4.3 \times 10^{19}$ a); however, its long half-live permits it to be considered a stable isotope.

2. Background

2.1. Calcium isotope basics and nomenclature

The Ca isotope ratio determinations of Russell et al. (1978) provide the basis for current measurements. Established on sample measurements where radiogenic ^{40}Ca/^{44}Ca excesses are negligible, these values are used to represent the normal terrestrial composition at about 0.01% precision. Modern ^{40}Ca/^{44}Ca and ^{43}Ca/^{44}Ca measurements of mafic achondrites and oceanic basalts by Simon et al. (2009) were used to reevaluate the initial terrestrial Ca isotopic composition. Assuming the normal ^{42}Ca/^{44}Ca = 0.31221 of Russell et al. (1978), the weighted means of these measurements yield ^{40}Ca/^{44}Ca = 47.1480 ± 0.0004 (2σ) and ^{43}Ca/^{44}Ca = 0.064868 ± 0.000001 (2σ) that are consistent with the previous determinations by Russell et al. (1978) showing that at the bulk rock scale many planetary materials exhibit a homogenous Ca isotopic composition. It should be noted that Simon et al. (2009) report a resolvable (+0.05 to +0.1‰) ^{40}Ca/^{44}Ca excess for the commonly used carbonate standard SRM915a.[5] More recently, and also at higher precision, ^{43}Ca/^{44}Ca, ^{46}Ca/^{44}Ca, and ^{48}Ca/^{44}Ca measurements show that some bulk meteorites exhibit resolvable ^{48}Ca/^{44}Ca anomalies (Dauphas et al., 2014a, Schiller et al., 2015, as discussed in more detail below).

For radiogenic enrichment and nucleosynthetic heterogeneity studies, non-mass-dependent Ca isotopic variations are commonly reported as ε^{x}Ca/^{44}Ca (equal to $10^4 \times (((^{4x}\text{Ca}/^{44}\text{Ca})_{\text{sample(N)}}/(^{4x}\text{Ca}/^{44}\text{Ca})_{\text{standard(N)}} - 1))$), where x is 40, 42, 43, 46, 48, and subscript N refers to internal normalization to ^{42}Ca/^{44}Ca = 0.31221 to remove both instrumental fractionation and mass-dependent fractionation intrinsic to the sample. The normalization value, however, is dependent on the choice of mass fractionation law, and the same law is not necessarily appropriate for both instrumental and intrinsic fractionation (see Zhang et al., 2014).

In the early literature, stable Ca isotope studies used δ^{40}Ca/^{44}Ca notation (equal to $10^3 \times ((^{40}\text{Ca}/^{44}\text{Ca})_{\text{sample}}/(^{40}\text{Ca}/^{44}\text{Ca})_{\text{standard}} - 1)$) as a measure of the natural isotopic variations, including both mass-dependent and non-mass-dependent, intrinsic to the sample. This notation has the somewhat confusing consequence that natural mass-dependent heavy isotope enrichments lead to negative delta values (Russell et al., 1978). Skulan et al. (1997) used the Russell et al. (1978) ratios as references for assessing natural mass-dependent isotopic variation, and introduced the δ^{44}Ca/^{40}Ca designation (equal to $10^3 \times ((^{44}\text{Ca}/^{40}\text{Ca})_{\text{sample}}/(^{44}\text{Ca}/^{40}\text{Ca})_{\text{standard}} - 1)$), which is more consistent with the notation used for other stable isotope systems, where the heavier isotope is in the numerator such that the high values for both the isotope ratio and delta value represent relative enrichment of heavy isotopes. This δ-notation is adopted by most recent stable Ca isotope studies; however, we note that this tradition is not strictly followed in literature as most non-mass-dependent Ca isotopic data for meteorite components are reported using δ-notation. It is important to note that the most abundant isotope, ^{40}Ca, is also one of the radioactive decay products of ^{40}K (half-life of ~1.25 Ga). δ^{44}Ca/^{40}Ca therefore includes potential radiogenic ingrowth of ^{40}Ca in the samples. This complication can be avoided by either measuring δ^{44}Ca/^{42}Ca and then converting to δ^{44}Ca/^{40}Ca by multiplying by approximately 2[6] (e.g., Huang et al., 2012; Fantle and Tipper, 2014; Valdes et al., 2014, 2019; Zhang et al., 2014; He et al., 2017; Amsellem et al., 2017, 2019), or by measuring ^{44}Ca/^{40}Ca directly and then correcting for radiogenic ^{40}Ca ingrowth using additional (unspiked) measurements when necessary.

In this review, when the terms "anomalous" or "variable" are used, we refer to mass-dependent isotopic compositions which, with consideration of their internal and external errors, depart from what is expected by mass-dependent fractionation and fall outside the range of values estimated for bulk Earth or the terrestrial standard referenced in the study. Regarding non-mass-dependent isotopic compositions, the terms refer to Ca isotopic compositions that fall outside the composition of a terrestrial standard. As analytical precision improves, subtle radiogenic enrichment effects in samples, and the propagation of poorly recognized isotopic artifacts in standard materials and those potentially produced during instrumental mass bias correction, need to be considered as possible explanations for observed Ca isotopic variation.

There are currently more than four different reference values commonly used in the modern literature for Ca isotope measurements (including CaF_2, Bulk Silicate Earth "BSE", modern seawater, and artificial calcium carbonates SRM915a and SRM915b). Although the SRM915a standard is no longer commercially available, it is presently still used in the majority of cosmochemical studies. Those studies that used BSE as a reference value have estimated its Ca isotopic composition relative to SRM915a ($\delta^{44}\text{Ca}/^{40}\text{Ca}_{\text{BSE-SRM915a}}$) in a number of ways. For example, Huang et al. (2010) modeled $\delta^{44}\text{Ca}/^{40}\text{Ca}_{\text{BSE-SRM915a}}$ from the Ca isotopic compositions of the principal Ca-bearing minerals in mantle peridotites. More recently, Kang et al. (2017) estimated $\delta^{44}\text{Ca}/^{40}\text{Ca}_{\text{BSE-SRM915a}}$ through the measurement of spinel and garnet lherzolites. The different approaches yield nearly identical values (+1.05 ± 0.04 vs. +0.95 ± 0.05, respectively; see Antonelli and Simon (2020) and discussion therein).

Here, +0.95 is adopted as the Ca isotopic composition of BSE relative to SRM915a because this estimate is based on a larger sample set. In order to facilitate inter-study comparison, all data discussed have also been converted to both SRM915a and BSE scales ($^{44}\text{Ca}/^{40}\text{Ca}_{\text{BSE}} = \delta^{44}\text{Ca}/^{40}\text{Ca}_{\text{SRM915a}} - 0.95$) in Supplementary Table 1. For the remainder of this review, SRM915a composition is referred to as "Earth" and data is discussed as referenced to SRM915a. For original data and conversion information, see Supplementary Table 1. Positive δ^{44}Ca/^{40}Ca indicate

[5] See similar reports discussed in the high-temperature geochemistry contribution (Antonelli and Simon, 2020) to this special issue.

[6] 2.05 for the canonical exponential mass law, 1.93 for the Rayleigh law which may be associated with kinetic isotopic fractionation, or 2.10 for the equilibrium mass law.

heavy isotopic compositions and negative $\delta^{44}Ca/^{40}Ca$ indicate light isotopic compositions. Non-mass-dependent data are referenced to the standard reported in the relevant reference, where the mass fractionation law and reference ratios reported are summarized in Supplementary Table 1. While it is possible that differences in reporting non-mass-dependent data may cause issues when comparing datasets, since non-mass-dependent data are always reported relative to a terrestrial standard, the subtle difference in the calculated mass fractionation corrected ε-values introduced by those different approaches is comparable or smaller than the reported analytical uncertainty.

2.2. Theoretical mass-dependent fractionation models

Theoretical and experimental studies provide a basis for understanding the stable isotopic composition of planetary materials, in particular isotope effects related to evaporation at low pressures (Esat et al., 1986; Davis et al., 1990; Grossman et al., 2000; Humayun and Cassen, 2000; Nagahara and Ozawa, 2000; Richter et al., 2002; Young et al., 2002; Zhang et al., 2014; Davis et al., 2015). Such studies imply that evaporative residues must have been heated at low pressures to produce appreciable mass-dependent isotopic fractionation (Esat et al., 1986; Davis et al., 1990; Young et al., 1998; Richter et al., 2002; Yamada et al., 2006; Richter et al., 2007; Shahar and Young, 2007; Knight et al., 2009; Zhang et al., 2014). As such, the heavy Mg and Si isotope enrichments of many CAIs require that they experienced evaporation at low pressures ($<10^{-4}$ bar), conditions that are thought to be typical near the proto-Sun. In contrast, the normal Mg and Si isotopic compositions reported in some parts of CAIs (Bullock et al., 2013; Simon et al., 2005) and for chondrules (Galy et al., 2000; Cuzzi and Alexander, 2006; Alexander et al., 2008) imply that these materials formed from high local partial pressures and/or dust-rich regions of the Solar nebula distinct from the hot inner Solar nebula. Thus, the degree of enrichment of heavier Mg and Si isotopes in disk materials provides evidence of heating and a record of the pressure, possibly due to the local concentration of solids under which they formed (Cuzzi and Alexander, 2006).

To test models for mass fractionation related to evaporation, it is useful to compare the refractory Ca isotopic signature in early formed solids to that of moderately volatile element isotopic signatures, such as Mg. Because of its highly refractory nature, Ca isotopic signatures record early mass-dependent isotope fractionation. In contrast, Mg isotopic records preserved in individual CAIs may be dominated by the last isotopic exchange event, overprinting the record of the earliest stages of nebular evolution.

Comparison of Ca and Mg isotopic data for CAIs (e.g., Niederer and Papanastassiou, 1984; Simon et al., 2017) and numerical models demonstrates the apparent inconsistency between Ca and Mg isotope effects (Fig. 1). There remains a limited number of samples in which Ca isotopes have been measured along with Mg, and many of these are FUN (Fractionated with Unknown Nuclear effect) inclusions. Because of the relatively large uncertainty (±3‰) in $\delta^{44}Ca/^{40}Ca$ ratios reported by early Ca isotope studies, more high precision measurements are needed to fully interpret the interrelationships between Ca and Mg effects in chondrite components. Though the analytical precision of Ca isotopes has significantly improved, it is worth noting that current mass spectrometry methods may require further refinement. This is especially true where large naturally occurring isotope fractionation that occurred during CAI formation may not follow an exponential fractionation law (e.g., Lee et al., 1979; Ireland et al., 1992). As such, current instrumental mass bias corrections could lead to apparent non-mass-dependent isotope anomalies (see Huang et al., 2012; Zhang et al., 2014). Nevertheless, published results support the hypothesis that enrichment of heavy Ca isotopes arose from extensive evaporation of CAIs (Zhang et al., 2014) followed by later addition of less fractionated Mg (see Fig. 1). This could be analogous to the "flash heating" hypothesis (Wark and Boynton, 2001) used to explain the formation of spinel-hibonite Wark-Lovering rim layers surrounding many CAIs. More generally, it is critically

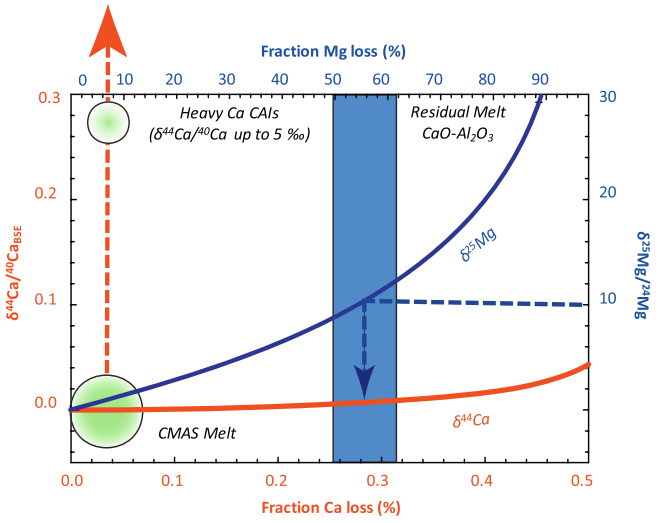

Fig. 1. Modeled Rayleigh-like isotope fractionation due to evaporation of CAI-like precursors; Ca-red and Mg-blue curves are calculated by Simon and DePaolo (2010). This work shows how CAIs with high $\delta^{44}Ca/^{40}Ca$ compositions record at least two and likely three distinct nebular events, the first involved extensive high temperature evaporation leading to Ca isotope fractionation, the second included significant Mg (and Si) addition, and the third involved additional evaporation leading to fractionated high $\delta^{25}Mg/^{24}Mg$ compositions. Complete (>99%) evaporative loss of Mg is implied by CAIs with high $\delta^{44}Ca/^{40}Ca$ compositions (off-scale) (Niederer and Papanastassiou, 1984) (i.e., heavier than all values of Ca-curve). Based on the fraction of Ca loss implied by the typical Mg isotopes of CAIs (i.e., upper range shown by blue column), minimal fractionation should exist. The models track changes in residual melt composition during evaporative loss of MgO, SiO_2, Al_2O_3, and CaO and match experiments of Richter et al. (2002). Once CaO and Al_2O_3 dominate the residue (≥80% Mg loss) evaporation rates of CMAS melts are less well understood and isotopic fractionation models that assume a constant evaporation coefficient for calcium (e.g., Simon and DePaolo, 2010; Shahar and Young, 2007; Richter et al., 2002; Young et al., 1998) match experiments less well. Calcium dominated evaporation experiments of Zhang et al. (2014) indicate ~4× greater Ca isotope fractionation, which is still broadly consistent with the models shown, but indicate the need for refined models that more accurately account for changing evaporation rates and the chemical species pertinent to evaporation of materials that are largely made of CaO and Al_2O_3. Simon and DePaolo (2010) define $\delta^{44}Ca/^{40}Ca = 0$ as the BSE composition, which has a value of +0.95 relative to the Ca standard SRM915a (see Section 2.1). For interpretation of the references to color in this figure legend, the reader is referred to the web version of this article.

important to understand the range of temperature conditions as well as the effects of open system isotopic exchange, because both have implications for the nebular settings in which chondrite components formed and evolved. Such insights may help reconcile some of the differences reported for Al-Mg chronologies between different nebular materials and studies (e.g., Simon and Young, 2011; MacPherson et al., 2012), and/or the observed abundances of various short-lived radionuclides. For example, this could help explain why the abundances of both ^{41}Ca and ^{26}Al tend to be correlated, but are unexpectedly absent in some CAIs (Goswami, 2004; Srinivasan et al., 1996; Liu, 2017). Integrating these isotopic signatures in nebular materials is essential to understand the connections between distinct nebular environments in space and time.

Kinetic isotopic fractionation effects during condensation and evaporation have been modeled (e.g., Humayun and Cassen, 2000; Simon and DePaolo, 2010; Simon et al., 2017). Simon et al. (2017) compiled studies with multi-element isotopic measurements of CAIs to test the latest condensation model. These comparisons help to evaluate the isotopic consequences of condensation from a nebular gas considering the kinetics of condensation, the degree of undercooling, and potential reservoir effects. While it is possible to directly measure

fractionation factors for evaporation (α_{evap}) in the laboratory, this is not the case for condensation fractionation factors (α_{cond}). Instead, a condensation model is needed to indirectly obtain α_{cond}. Invoking the law of mass action, Simon et al. (2017) showed that: $\alpha_{eq} = \frac{\alpha_{cond}}{\alpha_{evap}}$. Equilibrium fractionation factors can be calculated or measured experimentally, allowing one to solve for α_{cond} (Simon et al., 2017).

Kinetic isotopic fractionation during condensation depends upon the relative roles of collisional frequency (between gas species and the grain surface), compared to the ability of a gas species to incorporate into the condensed phase (Simon and DePaolo, 2010). Partition of the lighter isotopes into the condensates is favored when collisional frequency is the dominant controlling effect. In the nebula, the magnitude of fractionation is mainly controlled by both the speciation transformed from vapor to solid or vice versa, and the degree of evaporation or condensation. Zhang et al. (2014) showed experimentally that when an element, Ti in this case, has more than one significant evaporating species, this can be important (see Simon et al., 2017 for a worked example that accounts for both TiO and TiO_2 in the vapor phase). For Ca, one can assume a simpler scenario in which α_{eq}, for any given solid-vapor reaction, only has Ca in the vapor phase. This can be justified because at realistic nebular conditions Ca >> CaO in the vapor phase (Zhang et al., 2014).

Ultimately, the relative importance of equilibrium versus kinetic isotope effects in isotope fractionation depends on the degree of exchange "overstepping" as measured by the saturation index $S_i = P_i/P_{i,eq}$, with $S_i > 1$ implying condensation. S_i can be equated with a temperature difference (e.g., undercooling) from the equilibrium condensation temperature using the Van't Hoff equation and the enthalpy for the condensation reaction (Simon and DePaolo, 2010).

This model shows that for fractionation during condensation (Simon and DePaolo, 2010; Simon et al., 2017):

$\alpha_{cond} = \frac{\alpha_{eq}\alpha_{kin}S_i}{\alpha_{eq}(S_i-1)+\alpha_{kin}}$ where $\alpha_{kin} = \alpha_{evap}\alpha_{eq}\sqrt{\frac{m_i}{m_i'}}$ with m_i and m_i' being the masses of the lighter and heavier isotopes of the species of interest,

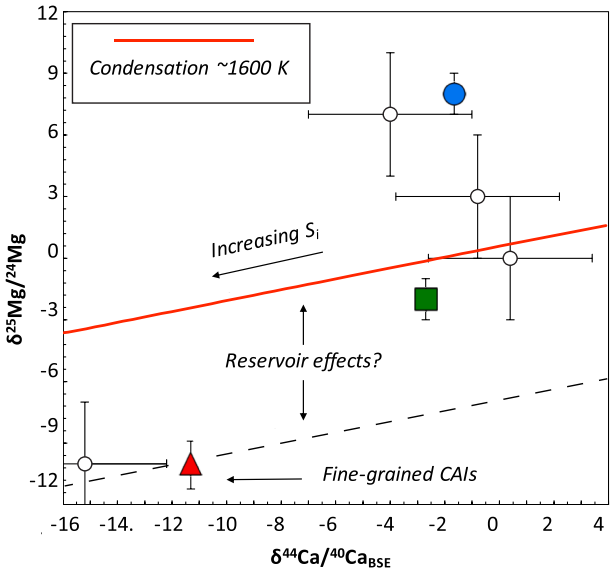

Fig. 2. $\delta^{44}Ca/^{40}Ca$ and $\delta^{25}Mg/^{24}Mg$ as a function of oversaturation (S_i) calculated from the condensation model of Simon et al. (2017). Double-spike Ca TIMS data (Simon et al., 2017; Huang et al., 2012) coupled with MC-ICPMS Mg data (Bullock et al., 2013; Jordan et al., 2013) for several CAIs (type B, blue circle; type B forsterite bearing, green square; and type A fine-grained, red triangle) and early data of Niederer and Papanastassiou (1984) (open circles) are shown. These authors define $\delta^{44}Ca/^{40}Ca = 0$ as the BSE composition, which has a value of +0.95 relative to the Ca standard SRM915a (see Section 2.1). For interpretation of the references to color in this figure legend, the reader is referred to the web version of this article.

respectively. A preliminary comparison of coordinated multi-element measurements can be made to the condensation model (Fig. 2). Other than showing that heterogeneity exists, the early TIMS data (open symbols) are insufficiently precise to constrain the model. The steadily growing data available (e.g., Huang et al., 2012; Simon et al., 2017; Bermingham et al., 2018), however, allows us to quantify the undercooling associated with condensation. Moreover, we see clear evidence that various CAI types formed from Mg isotopic reservoirs that are distinct from that which is "normal" to planetary bodies (see also Huang et al., 2012 and Bermingham et al., 2018, summarized in Section 3.2.6, for further information on this interpretation). We expect clarity on these promising findings when more precise measurements are made on a representative suite of CAIs.

3. Calcium isotope constraints on the origin of chondrite components

Early meteorite studies exploited the naturally high Ca concentrations in meteorite components to collect coupled mass-dependent and non-mass-dependent Ca isotopic data (e.g., Lee et al., 1978, 1979; Niederer and Papanastassiou, 1984; Ireland, 1990; Ireland et al., 1991, 1992). The elemental and isotopic compositions of chondrite components provided some of the first sample-based constraints on the thermal and chemical characteristics of the disk. Here, studies reporting Ca isotope ratios in chondrite components are reviewed and a synthesis of these data is presented. Although the emphasis of this review is on Ca isotopes, the significance of chondrite component Ca isotopic data in deciphering Solar System evolution is bolstered when interpreting the data in the context of Ti, Mg, and O isotopic data and rare earth element (REE) abundance data.

3.1. Refractory inclusions

Refractory inclusions are small (μm to cm) objects that are dominated by refractory Al, Ca, Ti, Mg, and Si oxides. Refractory inclusions in CM chondrites have higher abundances of hibonite and spinel compared to Ca-Al-rich silicates in CV chondrites (MacPherson et al., 1983). Rare earth elements are trace in abundance in refractory inclusions. Their relative fractionation patterns are highly variable as a result of the inclusions undergoing complex thermal processing in the disk prior to accretion to a parent body (e.g., Boynton, 1975; Davis and Grossman, 1979; Ireland, 1988). Based on mineralogy and elemental composition, refractory inclusions can be broadly grouped into the following types hibonite-bearing refractory inclusions, Ca-Al-rich silicate CAIs (Type 1 – VI[7]; Martin and Mason, 1974; Mason and Taylor, 1982), and ameboid olivine aggregates (AOAs).

3.1.1. Hibonite-bearing refractory inclusions

Hibonite-bearing refractory inclusions are smaller (μm-scale) than Ca-Al-rich silicate CAIs and AOAs (mm- to cm-scale); however, their isotopic variations can be an order of magnitude or more anomalous (Fig. 3). Hibonite-bearing refractory inclusions are predominantly found in CM2, but some have been found in CV3, CO3, CR, and H3 chondrites. These refractory inclusions preserve early disk chemistry because hibonite is predicted to be one of the first (after corundum) major element-bearing phases to condense from the Solar gas (Grossman, 1972; Davis et al., 1982) or it is the distillate of Solar gas evaporation (Ireland et al., 1992). There are at least five principal types of hibonite-bearing inclusions. These are distinguished on the basis of petrography and morphology. This includes Blue AGgregates (BAGs), hibonite-bearing spherules, HAL-type inclusions (HAL-type), PLAty hibonite Crystal fragments (PLACs), and Spinel-HIBonite spherules (SHIBs) (but see Kööp et al., 2016a for a description of some hibonite-rich objects in

[7] Group IV CAIs are mainly composed of chondrules.

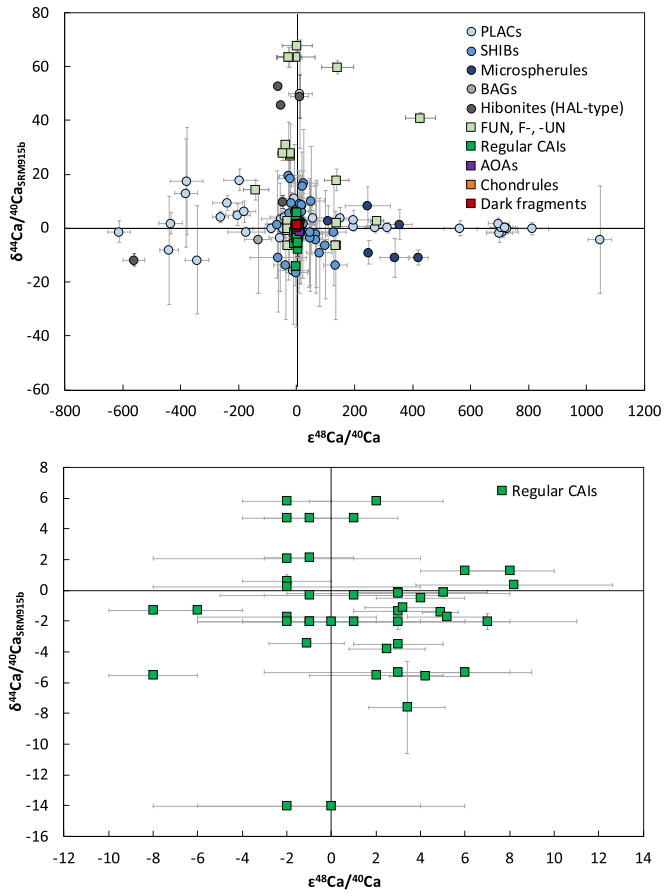

Fig. 3. Non-mass-dependent ($\varepsilon^{48}Ca/^{44}Ca$) *vs.* mass-dependent ($\delta^{44}Ca/^{40}Ca$) isotopic compositions obtained from the same meteorite component. Error bars are those reported in the original publications. Mass-dependent data reported relative to SRM915a. The area around the origin in (a) is shown in (b) and displays regular CAIs only. The reader is referred to the web version of this article for the color version of this figure.

Murchison which do not clearly fall into these morphological categories).

3.1.1.1. BAGs. Blue AGgregates are rare hibonite-rich refractory inclusions found in CM chondrites. They are pleochroic blue (as observed using an optical microscope) bladed hibonite crystal aggregates and comprise crystal plates and fragments. Blue AGgregates typically have similar TiO_2 (5.1 to 6.5%), low trace element abundances with large relative depletions in ultrarefractory elements (Group II-like patterns), and an absence of spinel (Ireland, 1988, 1990).

Only one BAG (13−23) has been documented for Ca isotopic compositions (Ireland, 1990). This inclusion does not display Ca or Ti isotope mass-dependent fractionation, but it is depleted in $\varepsilon^{48}Ca/^{44}Ca$ (-133 ± 47) and $\varepsilon^{50}Ti/^{48}Ti$ (-227 ± 31). Other BAGs that have been analyzed have similar depletions in ^{50}Ti; however, BAG 10–31 has a near-normal ^{50}Ti composition (Ireland, 1990). Inclusion 13–23 and other BAGs possess heavy mass-dependent Mg isotopic compositions ($\Delta^{25}Mg$[8]). Generally, mass-independent $\delta^{26}Mg$[9] isotopic compositions have been linked to in-situ decay of short-lived radioactive isotope ^{26}Al ($t_{1/2}$ ~0.7 Ma). Typically, BAGs have unresolved $\delta^{26}Mg$ compositions (e.g., BAG 13–23) from the standard, or are depleted in ^{26}Mg which could suggest some BAGs did not contain live ^{26}Al (Ireland, 1988, 1990; Liu et al., 2009). The combined isotope and trace element data are consistent with BAGs being condensates from a gas from which lower temperature components have been removed (Ireland, 1990). Given the rarity of BAGs and the absence of multi-element and isotopic datasets, however, the origin of these inclusions remains poorly constrained.

3.1.1.2. Hibonite-bearing spherules. Hibonite-bearing spherules comprise a rare subset of refractory inclusions identified in CM2, CO3, and CH3 meteorites (Ireland et al., 1991; Russell et al., 1998). These spherules contain hibonite and silicate glass, or are glass-free but contain hibonite and pyroxene. From Ireland et al. (1991) and Russell et al. (1998), hibonite-bearing spherules display a range of REE abundance patterns, including Group II patterns. Characteristically, hibonite-bearing spherules record large, coupled excesses in $\varepsilon^{48}Ca/^{44}Ca$ (up to +400) and $\varepsilon^{50}Ti/^{48}Ti$ (up to +200) in both glass and hibonite, where each phase is similarly enriched. There is an absence of Ca and Ti mass-dependent isotope fractionation, except for hibonite in one spherule (MUR7-228), which is slightly light ($\delta^{44}Ca/^{40}Ca$ -11 ± 3) (Ireland et al., 1991). Magnesium isotopes can be mass-fractionated (heavy, in both glass and hibonite) (Ireland et al., 1991). Generally, hibonite-bearing spherules are depleted in $\delta^{26}Mg$, which implies an absence of ^{26}Al; however, hibonite in MUR7-228 records evidence of ^{26}Al as an excess of $\delta^{26}Mg$ (Ireland et al., 1991). Because of the rarity of these inclusions, their petrogenesis remains unclear; however, they may have formed via melting of various precursors under disequilibrium conditions and rapid cooling after hibonite crystallization (Ireland et al., 1991). The large excesses in ^{48}Ca and ^{50}Ti suggests they formed early in the disk, prior to incorporation of ^{26}Al.

3.1.1.3. HAL-type refractory inclusions. Hibonite-bearing refractory inclusions are compositionally unusual hibonite-bearing inclusions. They include HAL (Hibonite ALlende, from Allende), DH-H1 (from Dhajala, H3), 7–404 and 7–971 (from Murchison), and Isna SP16 (from Isna, CO3.7). HAL-type inclusions have been studied extensively, where thus far HAL is the largest hibonite-bearing inclusion and is a FUN inclusion based on its highly anomalous O, Mg, Ca, and Ti isotopic compositions (e.g., Allen et al., 1979, 1980; Lee et al., 1979, 1980; Davis et al., 1982; Bischoff and Keil, 1984; Hinton and Bischoff, 1984; Fahey et al., 1987b; Hinton et al., 1988; Ireland et al., 1992; Russell et al., 1998; Sahijpal et al., 2000).

HAL-type inclusions display light (LREE) or heavy (HREE) REE enrichments, strong depletions in Ce and V or Yb, and they generally have low Mg and Ti concentrations compared to other hibonites (Fahey et al., 1987a; Hinton et al., 1988; Ireland et al., 1992; Russell et al., 1998). Samples HAL, DH-H1, 7–404, and 7–971 possess homogeneous non-mass-dependent depletions in $\varepsilon^{48}Ca/^{44}Ca$ (~ −50) (but Isna SP16 shows no variations in ^{48}Ca) and can be anomalous in $\varepsilon^{50}Ti/^{49}Ti$ (e.g., −40 (7–971) and +150 (HAL)) (Ireland et al., 1992; Russell et al., 1998). HAL-type inclusions show non-correlated enrichments in heavy Ca (up to $\delta^{44}Ca/^{40}Ca$ +53) and Ti isotopes[10] (up to F_{Ti} +19; Ireland et al., 1992; Russell et al., 1998). Mass-dependent Ti isotope fractionation is inversely correlated with Ti concentrations (Ireland et al., 1992). HAL-type inclusions tend to display low inferred initial $^{26}Al/^{27}Al$; however, Isna SP16 records a high initial $^{26}Al/^{27}Al$ (Lee et al., 1979; Fahey et al., 1987a; Ireland and Compston, 1987; Russell et al., 1998). Samples HAL, DH-H1, 7–404, and 7–971 are enriched in ^{16}O relative to the terrestrial

[8] $\Delta^{25}Mg$ refers to mass-dependent Mg isotopic compositions, where positive $\Delta^{25}Mg$ is defined as an enrichment in the heavy isotopes relative to terrestrial Mg (Ireland, 1988).

[9] $\delta^{26}Mg$ refers to non-mass-dependent Mg isotopic composition from which the radiogenic component from live ^{26}Al can be determined (Ireland, 1988) where canonical $^{26}Al/^{27}Al_0$ is ~5.3×10^{-5} (MacPherson et al., 1995; Jacobsen et al., 2008; Larsen et al., 2011).

[10] Following Ireland (1990), F_{Ti} is defined as $\Delta^{47}Ti$ deviations from the terrestrial $^{47}Ti/^{49}Ti$ (defined by Niederer and Papanastassiou, 1984). Note, subsequent publications report F_{Ti} is defined as $\Delta^{46}Ti$ deviations from the terrestrial $^{46}Ti/^{48}Ti$ (defined by Niederer and Papanastassiou, 1984).

mean, and display heterogeneous mass-dependent fractionation toward heavy O compositions (Lee et al., 1980; Ireland et al., 1992).

The origin of HAL and HAL-type inclusions is debated. Models suggest they are distillation residues (Lee et al., 1980; Ireland et al., 1992), or aggregates of condensate grains from a reservoir characterized by F and UN isotope signatures (Allen et al., 1980; Davis et al., 1982). Russell et al. (1998) concluded that the range in chemical and isotopic compositions of HAL-type inclusions suggests they formed by distillation of isotopically distinct mixtures of less refractory material. Regardless of the true formation process, the variety in composition displayed by these inclusions in different meteorites (CV3, CM2, CO3, and H3) indicates that HAL-type hibonites are samples from different compositional regions of the disk at different times (following Russell et al., 1998).

3.1.1.4. PLACs and PLAC-like CAIs. PLAty-Crystals (PLACs) are one of two predominant hibonite crystal morphologies found in CM chondrites (Ireland, 1988). The other type of morphology is hibonite intergrown with Al-Mg spinel (Spinel-HIBonite spherules, SHIBs), which are discussed in the following section. PLAC hibonites are colorless (as observed with an optical microscope), small (≤150 μm) broken crystal fragments which are likely from larger inclusions and possess a restricted (<2.7%) TiO_2 composition (Ireland, 1988; Kööp et al., 2016a).

PLACs and hibonite-rich CAIs ("PLAC-like CAIs") are primarily found in CM chondrites and have been studied in detail. They record distinct chemical and isotopic compositions compared to other refractory inclusions (e.g., Ireland, 1988, 1990; Ireland et al., 1989; Liu et al., 2009; Kööp et al., 2016a; Kööp et al., 2018a, 2018b). PLACs tend to be depleted in relatively volatile elements and display a decrease in HREE (e.g., Ireland et al., 1989; Ireland, 1990). A characteristic isotopic feature of PLACs is that they possess the most isotopically anomalous (for Solar System-derived materials) non-mass-dependent ^{48}Ca compositions ($\varepsilon^{48}Ca/^{44}Ca$ −600 to +800) and ^{50}Ti compositions ($\varepsilon^{50}Ti/^{48}Ti$ −700 to −170; note PLAC 13–13 has an anomalously high $\varepsilon^{48}Ca/^{44}Ca$ of +1040 and $\varepsilon^{50}Ti/^{48}Ti$ of +2730; Ireland, 1990; Kööp et al., 2016a). Most PLACs have the same mass-dependent Ca and Ti isotopic compositions as the terrestrial standard (e.g., Ireland, 1990; Kööp et al., 2016a). As mass-dependent Ca and Ti isotope effects are small, non-mass-dependent Ca or Ti isotopic compositions do not couple with mass-dependent Ca or Ti isotope fractionation. One PLAC (7–644) has $\delta^{44}Ca/^{40}Ca$ +50 ± 20 which is resolved from the standard composition, but its mass-dependent Ti isotopic composition is the same as the standard (Ireland, 1990). This hibonite grain may, however, be related to HAL-type hibonites as it has a depletion in Ce (Ireland, 1990). Oxygen isotopic compositions[11] range from $\Delta^{17}O$ −28 to −17‰ (see Kööp et al., 2016a for this most recent compositional range). There are no Mg-isotopic effects, indicating that PLACs did not reach high enough temperature to cause mass-dependent Mg isotope fractionation (Ireland, 1990). PLACs generally have low inferred initial $^{26}Al/^{27}Al$ indicating an absence of ^{26}Al (Ireland, 1988; Ireland, 1990; Kööp et al., 2016a).

There is a broad correlation between non-mass-dependent anomalies of ^{48}Ca, ^{50}Ti, and $\Delta^{17}O$. PLAC-like CAIs with the largest $\Delta^{17}O$ values tend to possess the most anomalous ^{48}Ca and ^{50}Ti compositions, while those with the lowest $\Delta^{17}O$ values have generally the least anomalous or normal ^{48}Ca and ^{50}Ti compositions (Kööp et al., 2016a). This may indicate a physical link between ^{48}Ca and ^{50}Ti carriers and a ^{16}O-poor reservoir, where the initial Solar nebula was isotopically heterogeneous with respect to ^{48}Ca and ^{50}Ti carriers and this region was also ^{16}O-poor (see Kööp et al., 2016a for details). A similar relationship is found in bulk meteorites (e.g., Yin et al., 2009; Warren, 2011; Dauphas et al., 2014a; Huang and Jacobsen, 2017). The correlation could be used to constrain the timing of the CO self-shielding process (Huang and Jacobsen, 2017). Alternatively, the correlation may imply local isotopic variability in the Solar nebula gas, or that PLACs equilibrated in a gas of an evolving isotopic composition (e.g., Krot et al., 2012). Based on the low inferred initial $^{26}Al/^{27}Al$ compositions, the PLAC-forming region may have existed prior to the incorporated of ^{26}Al, indicating these may be the earliest formed objects in the Solar System (Kööp et al., 2016a).

3.1.1.5. SHIBs. Common refractory inclusions in CM chondrites are "SHIBs", which are small (<160 μm), mineralogically complex grains dominated by hibonite and spinel. They possess variable TiO_2 hibonite concentrations <10%, and clinopyroxene and refractory metal nuggets are trace phases in some SHIBs (Ireland, 1988; Kööp et al., 2016b, 2018a, and references therein). There are at least five SHIB morphologies (bladed, compact, massive, spherule, crystal; Ireland, 1990). The REE patterns of SHIBs are variable (ultrarefractory-deleted, ultrarefractory-enriched, or unfractionated REE patterns) and may correlate with morphology (e.g., Ireland, 1990).

Generally, SHIBs do not to possess large non-mass-dependent or mass-dependent Ca or Ti isotope effects. If these isotopes are variable in SHIBs, they are usually ±10% of the terrestrial value (Zinner et al., 1986; Ireland, 1990; Kööp et al., 2016b, 2018a). Kööp et al. (2016b) determined that SHIBs have a nearly constant $\Delta^{17}O$ value (~ −23‰), and a generally high, near-canonical inferred initial $^{26}Al/^{27}Al$ although variability in $^{26}Al/^{27}Al$ exists (Ireland, 1990; Kööp et al., 2016b). Variability in $^{26}Al/^{27}Al$ may indicate variable ^{26}Al distribution in the SHIB-forming region (e.g., Fahey et al., 1987a; Ireland, 1988, 1990; Sahijpal et al., 2000; Liu et al., 2009). It has also been suggested, however, that variable $^{26}Al/^{27}Al$ in SHIBS is consistent with high temperature processing of refractory precursors that formed with initially approximately canonical $^{26}Al/^{27}Al$ ratios (Kööp et al., 2016b; Liu et al., 2019).

Generally non-anomalous Ca and Ti isotopic compositions and uniform ^{16}O isotopic compositions of the SHIB forming region must be reconciled with their variable $^{26}Al/^{27}Al$. This compositional profile may indicate that the SHIBs formed early in a region that achieved isotopic homogeneity in O, Ca, and Ti isotopes prior to the homogenous distribution of ^{26}Al, such that these inclusions record the admixing of live ^{26}Al into the disk under variable thermal processing conditions (following Liu et al., 2012; see Kööp et al., 2016b). As noted by Kööp et al. (2016b), however, SHIB formation during variable addition of ^{26}Al would result in supracanonical and subcanonical ratios and a negative correlation between non-mass-dependent isotopic compositions and ^{26}Al is predicted. As these effects are not observed, Kööp et al. (2016b) cautiously concluded that the subcanonical $^{26}Al/^{27}Al$ compositions likely resulted from the resetting of the ^{26}Al-^{26}Mg system. If so, the homogeneity of the O isotopic compositions would imply that a homogeneous ^{16}O-rich region persisted until at least ~0.7 Ma after formation of most CAIs, and SHIBs allow study of this phase of disk formation.

3.1.2. Ca-Al-rich silicate refractory inclusions

Ca-Al-rich silicate CAIs are found mainly (4–13 vol%) in carbonaceous chondrites CO > CV > CM > CK, in lower abundance (~1 vol%) in

Table 2
Typical REE patterns seen in silicate CAIs (from Mason and Taylor, 1982).

Group	REE fractionation pattern	Abundance (rel. to CI chondrite)
I	Relatively unfractionated (excepting a small positive Eu anomaly)	~10–15
II	Highly fractionated, with depletion of the heavy lanthanides (Gd-Er) and Eu, and positive Tm and Yb anomalies	< 1 to 20
III	Unfractionated (excepting negative Eu and Yb anomalies)	~20
IV	Relatively unfractionated	~2–4
V	Relatively unfractionated	~10–20
VI	Relatively unfractionated (excepting positive Eu and Yb anomalies)	~10–20

[11] $\Delta^{17}O$ refers to non-mass-dependent O isotopic compositions and is equivalent to $\delta^{17}O - 0.52 \times \delta^{18}O$ (Clayton, 1993).

CR > CI > CH > CB, and < 0.1 vol% in ordinary, enstatite-, K-, and R-chondrites (Krot et al., 2014). The CAI primary mineralogy is similar to the first phases that are predicted to condense from a hot gas of Solar composition (e.g., Yoneda and Grossman, 1995; for reviews see MacPherson et al., 2005 and MacPherson, 2014). The fractionated REE patterns of CAIs reflect multiple stages of evaporation and condensation of Solar nebular material in the disk (Table 2). These observations, coupled with the ancient age of CAIs (e.g., 4567.30 ± 0.16 Ma; Connelly et al., 2012), support the interpretation that CAIs are among the first condensates to form in the protoplanetary disk. The most widely used CAI classification scheme is based on the compositions of large (mm to cm-scale) silicate-bearing (with minor hibonite) CAIs from Allende because this meteorite is the most abundant in large CAIs and thus they have been studied in the most detail. According to the absolute and relative REE patterns of these CAIs, CAIs can be classified into one of six groups (Group I to Group VI; Mason and Taylor, 1982).

3.1.2.1. Silicate-bearing "regular" CAIs. Silicate-bearing inclusions, so-called "regular" CAIs, refer to those CAIs that are dominated by silicate mineralogy and with minor hibonite (Ireland et al., 1991). Many studies have investigated the Ca isotopic composition of mineral phases, acid leachates, and bulk rock samples of silicate-bearing CAIs from the CV and CM parent bodies (e.g., Niederer and Papanastassiou, 1979; Jungck et al., 1984; Niederer and Papanastassiou, 1984; Hinton et al., 1988; Weber et al., 1995; Sahijpal et al., 2000; Simon et al., 2009, 2017; Moynier et al., 2010; Huang et al., 2012; Chen et al., 2015; Amsellem et al., 2017; Bermingham et al., 2018; Schiller et al., 2018).

Refractory inclusions from Allende are considered to have condensed with approximately uniform $\Delta^{17}O$ values (~ −23‰) and canonical $^{26}Al/^{27}Al$ ratios. Smaller CAIs from other meteorite groups (thermally unequilibrated ordinary chondrites and carbonaceous chondrites) record variable ^{16}O and heterogeneous ^{26}Al (Krot et al., 2012). In CAIs from CV and CR chondrites, small and generally positive $\varepsilon^{48}Ca/^{44}Ca$ (<+10; e.g., Huang et al., 2012; Bermingham et al., 2018) and $\varepsilon^{50}Ti/^{47}Ti$ (+7 to +12; e.g., Trinquier et al., 2009; Davis et al., 2018; Torrano et al., 2019) anomalies have been measured. Mass-dependent Ca isotopic compositions of CAIs are variable but predominantly light. Two Allende CAIs contain small excesses in $\varepsilon^{40}Ca/^{44}Ca$ that correlate with excesses in $\varepsilon^{50}Ti/^{47}Ti$ and $\varepsilon^{135}Ba/^{136}Ba$, and deficits in $\varepsilon^{142}Nd/^{144}Nd$ and $\varepsilon^{144}Sm/^{154}Sm$ (Simon et al., 2009)

The non-mass-dependent Ca isotope anomalies may originate from the heterogeneous distribution of matter from either Type II or Type Ia supernovae (e.g., Simon et al., 2009; Moynier et al., 2010; Huang et al., 2012; Dauphas et al., 2014a; Chen et al., 2015; Huang and Jacobsen, 2017; Bermingham et al., 2018). Yet to be determined, however, are the number and type(s) of presolar ^{48}Ca carriers and the timing of their introduction into the Solar nebula.

Combining the mass-dependent Ca isotopic compositions with chemical signatures for the inclusions, Huang et al. (2012) observed that mass-dependent Ca isotopic compositions from bulk silicate-bearing CAIs correlate with REE abundance patterns. CAIs with Group II patterns tend to possess light $\delta^{44}Ca/^{40}Ca$ compositions compared to those with Group I patterns. Huang et al. (2012) interpreted these data to indicate that up to 3% of an ultrarefractory evaporation residue from a chondritic reservoir was segregated prior to the formation of these CAIs. Bermingham et al. (2018) applied this model to additional CAIs and AOAs samples from CV and CR meteorites. Some CAIs and AOAs followed the same trend documented by Huang et al. (2012). For those components that display unfractionated REE patterns, however, Bermingham et al. (2018) proposed they likely formed through the coaccretion of the evaporative residue and condensate following Group II CAI formation or the chemical and isotopic signatures were decoupled via disk or parent body alteration.

Although mass-dependent bulk CAI Ca isotope characteristics are largely consistent throughout the reported studies, Simon et al. (2017) observed intra-CAI Ca mass-dependent isotope zoning in an Allende CAI. These observations indicate that a refractory element can be isotopically fractionated at the scale of an inclusion. This possibility was suggested in the pioneering work by Niederer and Papanastassiou (1984) on Ca isotope studies in refractory inclusions; however, it was not confirmed until high precision mass spectrometry could be paired with micromilling techniques (Simon et al., 2017). Given these findings, isotopic variability within a meteorite component needs to be better documented to determine how accurately a bulk inclusion composition reflects the initial (presumably inner) CAI isotopic composition. This can be achieved, for example, by expanding the database for isotope zonation studies to quantify the extent of isotopic variation for different elements from core to rim.

3.1.2.2. Silicate-bearing FUN CAIs. Silicate-bearing inclusions include unusual FUN CAIs. These refractory inclusions are mineralogically indistinguishable from normal CAIs and are only identifiable using their isotopic compositions that are highly fractionated (e.g., $\delta^{44}Ca/^{40}Ca$ −6 to +68, most displaying heavy compositions), display large non-mass-dependent isotopic variations (e.g., $\varepsilon^{48}Ca/^{44}Ca$ −140 to +430), and have generally low inferred initial $^{26}Al/^{27}Al$ (e.g., Kööp et al., 2018b and references therein). Decoupling between the F and UN properties of FUN inclusions has been observed, where CAIs can show either highly mass-dependent fractionated compositions (F) or highly anomalous non-mass-dependent compositions (UN; e.g., PLACs and PLAC-like CAIs) (Wimpenny et al., 2014; Park et al., 2014, 2017; Kööp et al., 2018b). These studies also found that the inferred initial $^{26}Al/^{27}Al$ compositions are canonical in F inclusions but are low in UN inclusions. Where oxygen data are available, it appears as though CAIs with canonical $^{26}Al/^{27}Al$ ratios have approximately constant $\Delta^{17}O$ values (−23‰), whereas CAIs with low inferred initial $^{26}Al/^{27}Al$ ratios have variable $\Delta^{17}O$ values (Kööp et al., 2018b). Consequently, these highly variable compositions are likely a result of FUN-like inclusions forming over an extended period of time sampling different stages of disk evolution and contributions from the parental molecular cloud (e.g., Kööp et al., 2018b; Simon et al., 2019).

3.1.3. Amoeboid olivine aggregate refractory inclusions

Amoeboid olivine aggregates are olivine (forsterite)-rich with trace Fe-Ni metal. They are irregularly shaped inclusions found in carbonaceous chondrites in similar abundances to CAIs (Grossman and Steele, 1976; for a review see Krot et al., 2014). They are complex in their minor phase mineralogy, suggesting that they are aggregates of material that formed under a range of disk conditions (Ruzicka et al., 2012; MacPherson, 2014). This makes it difficult to link elemental and isotopic variations from bulk AOA analyses to their causation processes in the disk (Bermingham et al., 2018).

3.1.3.1. Ameboid olivine aggregates. Ameboid olivine aggregates have not been extensively studied for Ca isotopic compositions. Bermingham et al. (2018) analyzed five AOAs from Allende and reported similar variations to many regular CAIs, with small $\varepsilon^{48}Ca/^{44}Ca$ (<+10) isotope anomalies and generally light Ca mass-dependent isotopic compositions ($\delta^{44}Ca/^{40}Ca$ −0.95 to +0.72). There is no correlation between non-mass-dependent and mass-dependent Ca isotopic compositions. Type II REE patterns were recorded in some AOAs and this can correlate with light Ca isotopic compositions; however, this is not pervasive. When these compositions are decoupled, it is likely a result of non-equilibrium condensation of the primary Ca-bearing mineral phases. Bulk compositions may reflect an average REE and Ca isotopic composition of different mineral assemblages within the aggregate. Alternatively, the variable non-mass-dependent composition may indicate that AOAs formed over different regions or time periods of disk evolution. Isotopic and chemical zonation studies and bulk sample analyses on additional AOAs are required to evaluate these interpretations.

3.2. Other meteorite components (chondrules, dark fragments, dark inclusions)

Recent studies report Ca isotopic compositions from bulk samples of chondrules, AOAs, dark fragments, and dark inclusions from CV, CM, R- and O-chondrites (Amsellem et al., 2017; Bermingham et al., 2018; Schiller et al., 2018). Following publications on refractory inclusions, these recent studies take a multipronged approach to sample analysis by comparing the mineralogy, REE compositions, and isotopic compositions of aggregates to provide chemical contexts in which to interpret the Ca isotopic composition of these complex sample types.

3.2.1. Chondrules

Chondrules are small (mm-sized), silicate-rich spherical objects commonly found in chondrites. They are generally considered to form from flash heating/cooling events in the disk over a period of up to ~3 Ma after t_0 (e.g., Pape et al., 2019). Several chondrules from Allende have been studied for mass-dependent Ca isotopic effects, where Ca isotopic compositions can be either normal, slightly heavy, or slightly light relative to Earth ($\delta^{44}Ca/^{40}Ca$ + 0.53 to +1.59) (Amsellem et al., 2017; Simon et al., 2017; Bermingham et al., 2018, Schiller et al., 2018). Bermingham et al. (2018) noted that some Ca mass-dependent isotopic compositions do not correlate with REE patterns, which was interpreted to indicate the conditions that set the chemical signatures of the chondrules were not responsible for determining their Ca isotopic compositions. Three chondrule compositions may preserve the relationship between REE and Ca mass-dependent isotopic composition, where chondrules with Group I REE patterns and moderate Ca isotope fractionation accreted both the condensate and the ultrarefractory residue.

Non-mass-dependent Ca isotopic compositions have been obtained from chondrules in CV, R- and O-chondrites (Bermingham et al., 2018; Schiller et al., 2018). In general, the non-mass-dependent Ca isotopic compositions of chondrules are variable and exhibit small $\varepsilon^{48}Ca/^{44}Ca$ (<+12) isotope anomalies. Schiller et al. (2018) suggested that the variation in non-mass-dependent Ca isotopic composition may indicate a rapid change in the composition of the material of the protoplanetary disk during the ~1 Ma time period over which ordinary chondrite derived chondrules formed. Future studies combining age determination and Ca isotope analyses will be critical in evaluating this interpretation.

3.2.2. Dark fragments and dark inclusions

Dark fragments from R chondrites are considered to be among the most primitive R-lithologies (Bischoff et al., 2011). Dark inclusions from Allende (CV3) are lithic chondritic clasts that may have formed in the disk (Kurat et al., 1989) or on the CV parent body (Krot et al., 2000a). Neither the dark fragments nor the dark inclusions possess variations in non-mass-dependent Ca isotopic compositions (Bermingham et al., 2018). These samples, however, display slightly heavy Ca isotopic compositions ($\delta^{44}Ca/^{40}Ca$ +1.26 to +1.33), indicating that they likely do not sample materials with highly variable Ca isotopic compositions and thus are not aggregates of direct nebular condensates. The Ca isotopic compositions support the interpretation that the inclusions formed in situ on the parent body as a variably altered fragment of the CV3 parent body lithology (Krot et al., 2000a). From Bermingham et al. (2018), the Ca isotopic composition of some dark inclusions may have been reset during parent body-based aqueous alteration events after lithification and aggregation of the inclusions. During alteration, diffusion-driven Ca isotope exchange reactions (for details, see Krot et al., 2000b) between the surrounding matrix and the inclusions may have occurred and resulted in the formation of Ca-rich rims. During these reactions, Ca isotopic compositions would become progressively lighter in the rim-deposits (see Section 2.2 for details on Ca isotope effect during diffusion). Isolation of inclusions from the matrix resulted in the removal of rim material and thus likely biased the bulk Ca isotopic composition recorded to the heavier core compositions. Future chemical and isotopic zonation studies that pair high precision mass spectrometry with micromilling techniques (following Simon et al., 2017) would provide the means to test this hypothesis and constrain the process(es) that fixed the Ca isotopic composition of Allende dark fragments.

3.3. Synthesis of meteorite component Ca isotopic data

Reconciling chemical and isotopic data from all types of chondrite components to produce a coherent model of protoplanetary disk evolution is challenging because many studies do not consistently generate coupled chemical and multi-isotopic (e.g., Ca, Ti, O, Mg-Al, and REE) datasets. To date, the chemical and isotopic data reviewed above indicates that the disk was isotopically and chemically heterogeneous over space and time.

Bermingham et al. (2018) attempted to constrain the origin of Ca isotopic variations in the disk by contrasting the Ca mass-dependent and non-mass-dependent isotopic compositions of different components. Non-mass-dependent isotope effects are generally considered to be the result of poorly mixed presolar carrier phases throughout the disk; however, debate remains regarding the process by which these grains became heterogeneously distributed in the disk. It has been posited that non-mass-dependent Ca isotopic heterogeneity is the result of two-component mixing of an anomalous endmember component (e.g., Type Ia or Type II supernova) with a Solar component (Simon et al., 2009; Chen et al., 2011; Huang et al., 2012; Dauphas et al., 2014a; Chen et al., 2015; Wasserburg et al., 2015; Huang and Jacobsen, 2017).

Thermal processing of multiple carrier phases has been proposed as an alternative interpretation (Schiller et al., 2015). If high enough temperatures were reached during thermal processing events, preferential removal of light Ca isotopes would have occurred, leaving an isotopically heavy and isotopically anomalous ^{48}Ca residue (Bermingham et al., 2018). This effect may be apparent when comparing non-mass-dependent and mass-dependent Ca isotopic compositions, where heavy isotope signatures would be coupled with more anomalous non-mass-dependent compositions, thus a positive $\delta^{44}Ca/^{40}Ca$ and $\varepsilon^{48}Ca/^{44}Ca$ correlation was predicted.

A recent investigation of this relationship indicated that mass-dependent and non-mass-dependent Ca isotopic compositions in nine "regular" silicate-bearing CAIs were not linearly coupled, although light $\delta^{44}Ca/^{40}Ca$ compositions were generally coupled with enrichments in $\varepsilon^{48}Ca/^{44}Ca$ (Bermingham et al., 2018). From a preliminary investigation (see Fig. 3), a simple correlation is absent when comparing Ca isotopic compositions of meteorite components. Davis et al. (2018) found no relationship between mass-dependent and non-mass-dependent fractionation for Ti isotopes in 46 Allende CAIs, even though there is a significant range in both mass-dependent and non-mass-dependent fractionation among CAIs. Thus, the lack of such a ubiquitous relationship for Ca isotopes is perhaps not surprising, but the reason remains unclear. To determine the relationship between mass-dependent and non-mass-dependent isotopic compositions coupled datasets are required. Extending this test to other chondrite components is most judiciously done by comparing datasets that report coupled mass-dependent and non-mass-dependent data from the same samples, using the same mass fractionation laws and normalization schemes, and data collected using similar analytical methods.

Similar to the trend noted by Ireland (1990), there is a continuum in the degree of $\varepsilon^{48}Ca/^{44}Ca$ heterogeneity between CAIs-types: PLAC/FUN > hibonite-bearing spherules > SHIB > regular CAIs > AOAs/chondrules. Additionally, systematic relationships are apparent among chondrite components: (1) PLACs record the most extreme enrichments and depletions in $\varepsilon^{48}Ca/^{44}Ca$ compositions of Solar System-derived materials, yet mass-dependent Ca isotope fractionation is absent. (2) FUN (including F, UN) and HAL-type possess large excesses and depletions in $\varepsilon^{48}Ca/^{44}Ca$ and these inclusions are predominantly heavy in mass-dependent Ca isotopic composition. (3) Hibonite-bearing spherules generally record large excesses in $\varepsilon^{48}Ca/^{44}Ca$ compositions, whereas mass-dependent Ca isotope fractionation is not evident. (4)

SHIBs possess moderate (6 to 10 times less anomalous than PLACs) non-mass-dependent Ca isotope anomalies; however, some PLACs have similar Ca isotopic compositions as SHIBs. (5) Silicate-bearing "regular" CAIs are dominated by relatively small excesses in $\varepsilon^{48}Ca/^{44}Ca$ which are commonly coupled with light mass-dependent Ca isotopic compositions.

The absence of resolved mass-dependent Ca isotope fractionation in PLACs and microspherules suggests that if thermal processing event(s) produced non-mass-dependent Ca isotope anomalies, they did not concurrently establish the observed mass-dependent effects. The fact that in some FUN CAIs large excesses or depletions in $\varepsilon^{48}Ca/^{44}Ca$ are coupled with large heavy mass-dependent fractionation suggests there may be a causal relationship between the two effects, but this is not ubiquitous because the relationship is not seen in all FUN, F, or UN CAIs. The Ca isotope systematics change in regular CAIs where positive $\varepsilon^{48}Ca/^{44}Ca$ anomalies are predominately coupled with light Ca isotopic compositions (Fig. 3b). Given that "regular" CAIs have the light Ca effects, it is possible that these CAIs formed from the fractionated gas that was enriched in light Ca isotopes imparted from earlier fractionation.

Studies that couple Ca isotopic compositions with chemical and isotopic data of other elements which record thermal processing events in the disk (e.g., REE, and O-, Al- and Ti- isotopic data) are required to determine how the Ca isotopic composition of meteorite components originate. This multi-element approach to analyzing chondrite components will also provide constraints that directly inform the following fundamental questions in cosmochemistry: (1) what were the combination and timing of stellar precursors into the Solar nebula; (2) what is the significance of non-mass-dependent isotopic compositions of refractory inclusions regarding mixing processes and location of these reservoirs in the disk? and (3) are non-mass-dependent compositions linked to mass-dependent isotopic compositions?

4. Planetary building blocks: bulk chondrites and achondrites

The building blocks of the Earth may be found in our meteorite collection; thus, studying meteorites in detail can provide insight into how a life-bearing planet evolved. This section surveys constraints provided by the Ca isotopic compositions of bulk chondrites and achondrites on the material that accreted to form the Earth, the Moon, and Mars.

4.1. Introduction to bulk meteorite samples

Bulk meteorites are useful for evaluating the genetic relationships between parent bodies that formed from isotopically distinct reservoirs in the disk (e.g., Chambers, 2001; Drake and Righter, 2002; O'Brien et al., 2006; Warren, 2011). Isotopic variations among bulk meteorites can be used to constrain the chemical nature of Earth's accretionary assemblage and to link this assemblage to distinct formation locations within the protoplanetary disk (Rubin and Wasson, 1995; Wasson and Kallemeyn, 1988; Wood, 2005; Raymond et al., 2009).

Chondrites have been divided into distinct classes that are defined primarily by their bulk chemical compositions, and secondarily by parameters such as mineralogy, oxygen isotopic composition, and chondrule abundance (Brearley and Jones, 1998; Weisberg et al., 2006; Krot et al., 2014). Most chondrites fall into one of three main classes (carbonaceous, ordinary, and enstatite). CI chondrites are the most chemically primitive meteorites as they have compositions—volatile elements excluded—similar to the Solar photosphere (e.g., Orgueil CI; Anders and Grevesse, 1989; Palme et al., 2014; Lodders, 2020). Carbonaceous chondrites, however, are by no means unaltered, as some have undergone extensive aqueous alteration (e.g., Zolensky and McSween, 1988; Brearley, 2006). Some members of the carbonaceous chondrite group contain the highest volatile element content compared to the Earth (e.g., Bland et al., 2005; Bermingham et al., 2020); thus, they are inferred to have originated from asteroidal parent bodies that accreted far from the Sun (Gradie and Tedesco, 1982).

Ordinary chondrites are also rich in volatiles compared to the Earth, but to a lesser extent than most carbonaceous chondrites (Palme et al., 2014; Scott and Krot, 2014), and they feasibly derive from parent bodies formed in the inner asteroid belt (Binzel, 1996). In enstatite chondrites, iron exists mainly in its metallic form or as a sulfide, in contrast to carbonaceous and L- and LL-type ordinary chondrites, where Fe is mostly present in oxides. The high metal content and low oxygen fugacity of enstatite chondrites indicates these meteorites formed in reduced part of the disk, possibly in the inner Solar System (Krot et al., 2014; Palme et al., 2014; Scott and Krot, 2014).

Achondrite meteorites sample the silicate crust and mantle of parent bodies that reached temperatures high enough to induce partial or wholesale melting (including 4-Vesta, the ureilite parent body, the Moon, and Mars). As such, achondrites present an opportunity to study the Earth's accretion of planetesimals that had already differentiated to some degree (e.g., Kleine et al., 2005; Kruijer et al., 2014). Chemical and isotopic analyses along with dynamical simulations have suggested that the parent bodies of achondrites possibly accreted earlier and closer to the Sun than the parent bodies of chondrites and some iron meteorites (e.g., Wasson and Wetherill, 1979; Grimm and McSween Jr., 1993; Kleine et al., 2005; Bottke et al., 2006; Warren, 2011). Thus, through the analysis of achondrites and chondrites different regions of the protoplanetary disk can be probed.

Most current models propose that the Earth accreted from a heterogeneous mixture of chondritic and achondritic precursors that formed at different heliocentric distances; however, the relative proportion of each precursor type remains debated (e.g., Drake and Righter, 2002; Fitoussi et al., 2016; Dauphas, 2017; Liebske and Khan, 2019). It has been argued that reduced, non-carbonaceous material (including achondrites) dominated the early part of Earth's main accretion history, while more oxidized, volatile-rich carbonaceous chondrite-like material accreted toward the end of Earth's formation (e.g., Schönbächler et al., 2010; Rubie et al., 2015; Grewal et al., 2019). It is feasible that the transition occurred at the time of the Moon-forming impact (e.g., Schönbächler et al., 2010). To a first approximation, however, Earth's bulk elemental composition is chondritic as the relative proportions of non-volatile elements in BSE are close to those found in chondrites (the so-called "chondritic Earth" model; Larimer, 1971; Kargel and Lewis, 1993; Palme and O'Neill, 2014).

4.2. Non-mass-dependent Ca isotopic variations among chondrite groups

The discovery of large Xe and Ne isotopic anomalies in carbonaceous chondrites (Reynolds and Turner, 1964; Black and Pepin, 1969; Lewis et al., 1975) and $\Delta^{17}O$ heterogeneity among meteorites and their components (Clayton et al., 1973) challenged the paradigm that the Solar System formed out of an initially homogeneous gas cloud (e.g., Cameron, 1962). Because these anomalies could not be linked to fission, spallation or Solar wind implantation, they were interpreted to derive from stellar lineage and, therefore, predate the Solar System. The subsequent identification of diamond (Lewis et al., 1987), silicon carbide (Bernatowicz et al., 1987; Zinner et al., 1987), and graphite (Amari et al., 1990) presolar grains as the host phases of noble gas anomalies provided evidence that presolar isotopic diversity had survived the nebula phase and was preserved in meteorites in the form of presolar grains.

The idea of early Solar nebula heterogeneity was further strengthened by the detection of non-mass-dependent isotopic effects in major rock-forming elements, including Ca, in CAIs and other refractory chondrite components (e.g., Lee et al., 1978, 1979; Niederer and Papanastassiou, 1984; see Section 3). Technical refinements and improvements in analytical sensitivity of TIMS and MC-ICP-MS permitted expansion of sample types that could be measured. This resulted in a shift of focus from refractory inclusions to bulk meteorites. Detection of non-mass-dependent effects in bulk meteorites showed that the heterogeneous distribution of Ca isotopes was preserved at the planetary scale

(Simon et al., 2009; Chen et al., 2011; Dauphas et al., 2014a; Bermingham et al., 2018). This demonstrated the utility of Ca isotopes for probing the genetic relationship between meteorite groups, the Earth, and other rocky planets, because they ostensibly formed in (isotopically) distinct regions of the disk (Dauphas, 2017).

Initially, only two bulk Ca isotopic measurements had been published, both on Allende (Niederer and Papanastassiou, 1979, 1984). Anomalous $\varepsilon^{46}Ca/^{44}Ca$ (−140) and $\varepsilon^{48}Ca/^{44}Ca$ (−29) were detected by Niederer and Papanastassiou (1979) but not Niederer and Papanastassiou (1984). Later, Simon et al. (2009) measured $\varepsilon^{40}Ca/^{44}Ca$ and $\varepsilon^{43}Ca/^{44}Ca$ variations in a suite of enstatite, ordinary, and carbonaceous chondrites. In this study, measurement uncertainties are generally too large to resolve chondrite compositions from Earth; however, carbonaceous chondrites Murray (CM2) and Vigarano, and ordinary chondrites St. Severin (LL6) and Dhajala show $\varepsilon^{40}Ca/^{44}Ca$ and $\varepsilon^{43}Ca/^{44}Ca$ enrichments of +0.3 to +2.3 relative to Earth (Fig. 4). These data indicate that the isotopic reservoirs sampled by carbonaceous and ordinary chondrites are distinct from that of the dominant component of Earth's building blocks. Moynier et al. (2010) corroborated these results by showing that Dhajala is distinct from Earth, with anomalous $\varepsilon^{40}Ca/^{44}Ca \sim +2$ and $\varepsilon^{43}Ca/^{44}Ca \sim +0.5$. In addition to data for $\varepsilon^{40}Ca/^{44}Ca$ and $\varepsilon^{43}Ca/^{44}Ca$, Moynier et al. (2010) presented data for $\varepsilon^{46}Ca/^{44}Ca$ and $\varepsilon^{48}Ca/^{44}Ca$: anomalies in $^{46}Ca/^{44}Ca$ can not be resolved, but Dhajala, Murray, and Vigarano have distinct $\varepsilon^{48}Ca/^{44}Ca$ from Earth with enrichments of up to +4.

Dauphas et al. (2014a) identified enrichments in $\varepsilon^{48}Ca/^{44}Ca$ between +2 to +4 in CI, CO, and CV chondrites. The authors also measured ordinary chondrites (LL, L and H); however, these are indistinguishable from Earth. Likewise, enstatite chondrites Adhi Kot (EH) and Jajh (EL) are also within analytical uncertainty of Earth (Fig. 4). The results of Huang and Jacobsen (2017) supported these findings as no discernable $\varepsilon^{40}Ca/^{44}Ca$ or $\varepsilon^{43}Ca/^{44}Ca$ anomalies could be detected in a suite of nine chondrites (CI, CM, CV, L, H, and EH) relative to Earth at the ±1 and ± 2 ε-unit levels, respectively. This study did not report $\varepsilon^{48}Ca/^{44}Ca$ anomalies in enstatite chondrites and ordinary chondrites, though all carbonaceous chondrite types were shown to possess $\varepsilon^{48}Ca/^{44}Ca$ excesses between +2 and +3. Yokoyama et al. (2017) presented data for seven ordinary chondrites, four of which possess small but resolvable $\varepsilon^{40}Ca/^{44}Ca$ excesses, where the largest anomaly is recorded by Bhola (LL3) ($\varepsilon^{40}Ca/^{44}Ca$ +2.5).

By obtaining an order of magnitude higher precision than previous studies, Schiller et al. (2015) reported non-mass-dependent $^{43}Ca/^{44}Ca$, $^{46}Ca/^{44}Ca$, and $^{48}Ca/^{44}Ca$ effects in ordinary and carbonaceous chondrites. One ordinary chondrite (Bovedy, L3) records $\varepsilon^{43}Ca/^{44}Ca$ and $\varepsilon^{46}Ca/^{44}Ca$ compositions that are unresolvable from Earth but also a $\varepsilon^{48}Ca/^{44}Ca$ depletion of −0.35. Ivuna (CI) is enriched in $\varepsilon^{43}Ca/^{44}Ca$ (+0.11), $\varepsilon^{46}Ca/^{44}Ca$ (+0.96), and $\varepsilon^{48}Ca/^{44}Ca$ (+2.06) relative to Earth. Schiller et al. (2018) also showed that the $\varepsilon^{48}Ca/^{44}Ca$ compositions of ordinary and carbonaceous chondrites (including CI, CM, CR, C2-ungrouped) do not overlap with that of Earth. The $\varepsilon^{48}Ca/^{44}Ca$ depletion in ordinary chondrites (−0.35 to −0.25) and excess in carbonaceous chondrites (+2.06 to +3.14) are similar to that reported in Schiller et al. (2015).

4.2.1. Earth's building blocks constrained by non-mass-dependent Ca isotopes in chondrites

That the Ca isotopic compositions of carbonaceous chondrites and ordinary chondrites are anomalous relative to Earth indicates that these meteorite types likely do not make up a significant proportion of Earth's precursor material. In contrast, the lack of non-mass-dependent Ca isotopic effects in enstatite chondrites suggests that the Earth and the enstatite chondrite parent body formed from a similar isotopic reservoir in the disk. These findings place Ca on the growing list of elements that display isotopic similarity between Earth and enstatite chondrites but not between the Earth and other meteorite groups— this includes O,[12] Si, Ni, Ti, Cr, Sr, Zr, Ru, and Ba (O: Clayton, 2004; Ni: Regelous et al., 2008; Ti: Trinquier et al., 2009; Cr: Qin et al., 2010; Sr: Moynier et al., 2012; Zr: Akram et al., 2015; Ru: Fischer-Gödde et al., 2015, Bermingham and Walker, 2017; Ba: Bermingham et al., 2016).

Using models based on mixing calculations, Dauphas et al. (2014a) and Dauphas (2017) demonstrated that Earth's $\Delta^{17}O$, $\varepsilon^{48}Ca$, $\varepsilon^{50}Ti$, $\varepsilon^{54}Cr$, $\varepsilon^{64}Ni$, and $\varepsilon^{92}Mo$ isotopic composition cannot be reproduced unless the proportion of enstatite chondrites in bulk Earth is >90%. Accretion of significantly less enstatite chondrite material yields a mismatch between the Earth and calculated isotope mixtures for one or more of the elements. The non-mass-dependent O, Ca, Sr, Ti, Cr, Ni, Zr, Ru, Ba, and Mo isotopic similarity between the Earth and enstatite chondrites supports the interpretation that the Earth primarily accreted material with approximately the same isotopic composition as that sampled by enstatite chondrites (Dauphas et al., 2014a; Dauphas, 2017).

How closely enstatite chondrites are related to Earth, however, has long been the subject of debate (e.g., Javoy and Pineau, 1983; Javoy, 1995; Javoy et al., 2010). The discussion focuses on the fact that, though enstatite chondrites and Earth resemble each other isotopically, they have very dissimilar elemental compositions. In particular, enstatite chondrites are depleted in FeO, enriched in volatiles, and have Si/Mg ratios higher than BSE (Wasson and Kallemeyn, 1988; Allègre et al., 1995). It may be that Earth and enstatite chondrites formed from the same parental nebular reservoir but experienced different condensation processes (Jacobsen et al., 2013; Dauphas et al., 2014a; Dauphas, 2017; Huang and Jacobsen, 2017). Experimental data and numerical modelling that simulates the condensation processes responsible for the observed differences in element composition are required to evaluate the validity of this hypothesis. Presently, however, non-mass-dependent Ca isotopic data support the hypothesis that the Earth formed primarily from material similar to enstatite chondrites.

4.3. Mass-dependent variation among chondrite groups

Early studies determined that the $\delta^{40}Ca/^{44}Ca$ signatures of bulk carbonaceous, ordinary, and enstatite chondrites (represented by CI, H6, and EH types: Russell et al., 1978; CV: Niederer and Papanastassiou, 1979, 1984) were indistinguishable from Earth, with no systematic variation in $^{40}Ca/^{44}Ca$ by chondrite type. More recent data indicates that some $^{44}Ca/^{40}Ca$ variation does, in fact, exist among chondrite groups, and between chondrite groups and Earth, at the <0.1‰ level of precision (Fig. 5). Specifically, carbonaceous chondrites possess $\delta^{44}Ca/^{40}Ca_{CI}$ +0.42 to +1.13, $\delta^{44}Ca/^{40}Ca_{CM}$ +0.55 to +0.84, $\delta^{44}Ca/^{40}Ca_{CO}$ +0.77 to +1.19, $\delta^{44}Ca/^{40}Ca_{CV}$ +0.10 to +0.78, ordinary chondrites display $\delta^{44}Ca/^{40}Ca_{LL,L,H}$ +0.91 to +1.16, and enstatite chondrites display $\delta^{44}Ca/^{40}Ca_{EH,EL}$ +0.90 to +1.54 (Simon and DePaolo, 2010; Valdes et al., 2014; Schiller et al., 2015; Amsellem et al., 2017; Huang and Jacobsen, 2017; Simon et al., 2017). Notably, analytically resolvable differences in $\delta^{44}Ca/^{40}Ca$ have also been reported in the same meteorite sample measured by different groups—for example, in Allende, Murchison (CM2), Orgueil, Abee (EH4), Indarch (EH4), and Qingzhen (EH3), as noted by Valdes et al. (2014) and Bermingham et al. (2018).

Generally, studies agree that carbonaceous chondrites are enriched in light Ca isotopes relative to Earth and ordinary chondrites have $^{44}Ca/^{40}Ca$ compositions that are indistinguishable from Earth (Simon and DePaolo, 2010; Huang and Jacobsen, 2017; Valdes et al., 2014;

[12] Proposals for the origin of meteoritic O isotopic variations now include photochemical effects (Clayton, 2002) and non-mass-dependent chemical effects (Thiemens and Heidenreich, 1983).

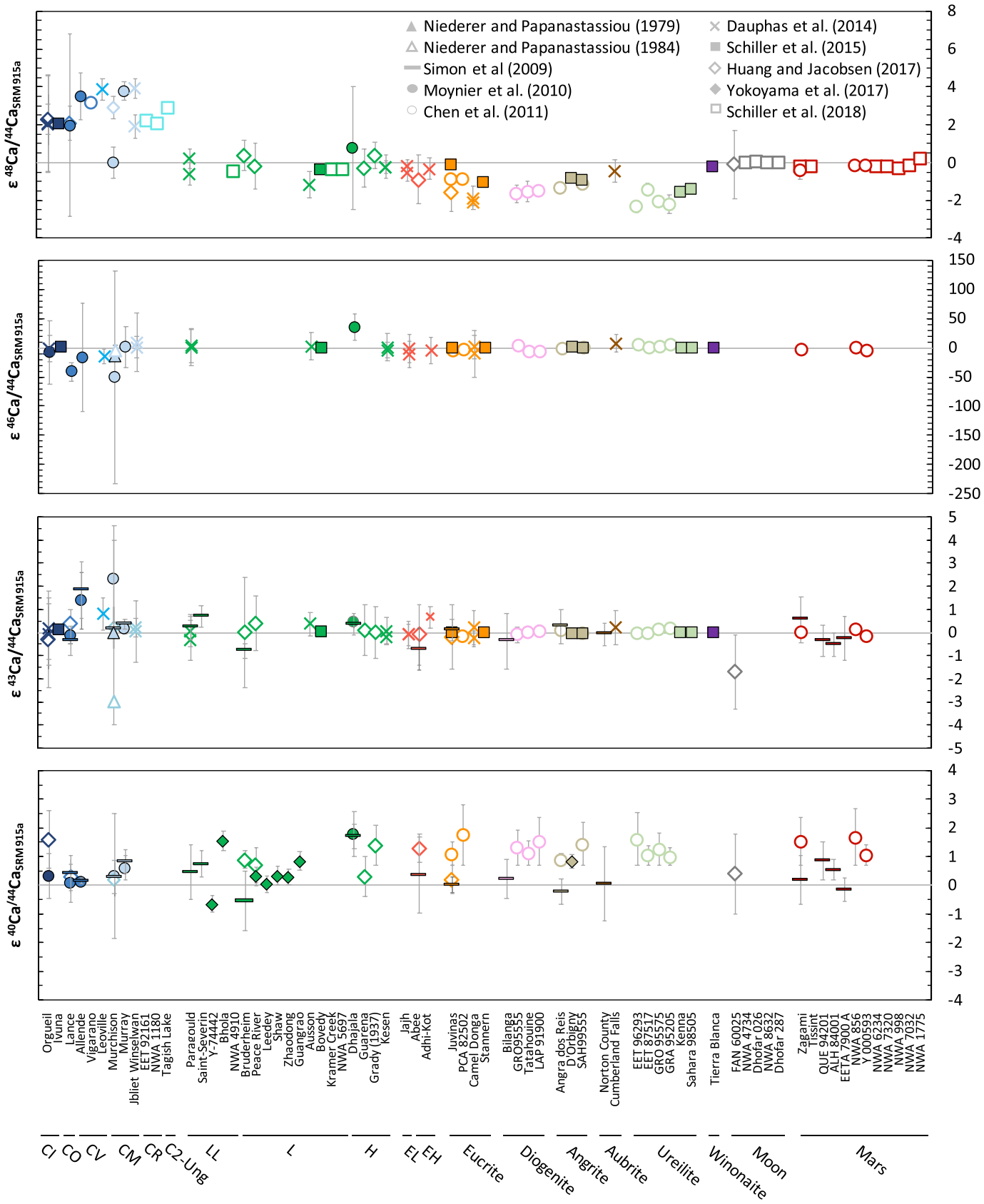

Fig. 4. Non-mass-dependent $\varepsilon^{40}Ca/^{44}Ca$, $\varepsilon^{43}Ca/^{44}Ca$, $\varepsilon^{46}Ca/^{44}Ca$, and $\varepsilon^{48}Ca/^{44}Ca$ isotopic compositions of chondrites, achondrites, lunar samples, and Martian samples. Error bars are those reported in the original publications. Error bars smaller than data points are not shown. The reader is referred to the web version of this article for the color version of this figure.

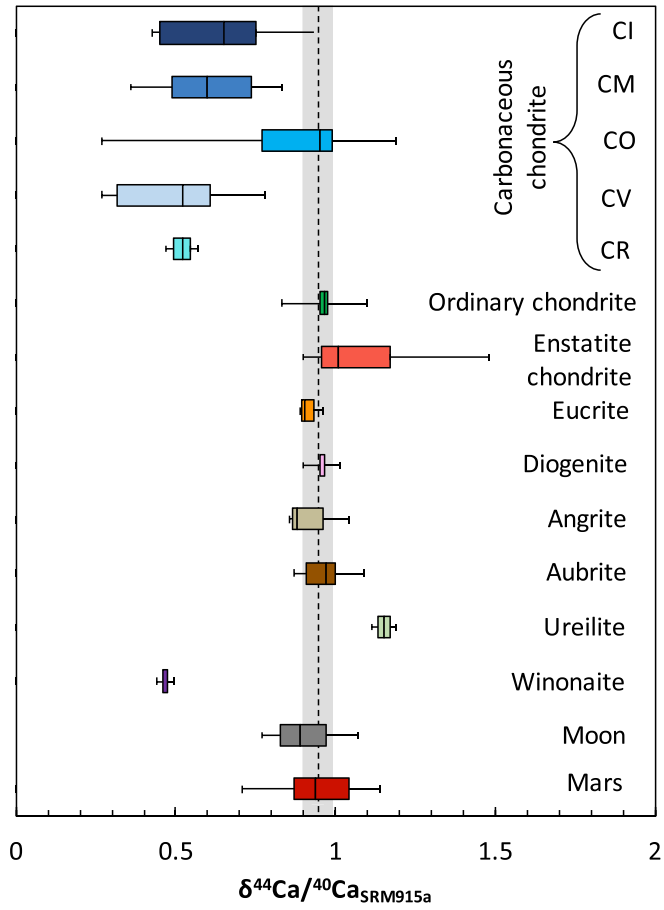

Fig. 5. Mass-dependent $\delta^{44}Ca/^{40}Ca$ compositions of chondrites, achondrites, lunar samples, and Martian samples. All data have been renormalized to Ca standard SRM915a. Boxes represent the spread of data about the median and the "error bars" indicate outliers. Data are from Niederer and Papanastassiou (1979, 1984), Simon and DePaolo (2010), Valdes et al. (2014), Magna et al. (2015), Schiller et al. (2015), Amsellem et al. (2017), Huang and Jacobsen (2017), Simon et al. (2017), Bermingham et al. (2018), and Schiller et al. (2018). The dotted line and grey band represent the BSE estimate of Kang et al. (2017), 0.95 ± 0.05. The reader is referred to the web version of this article for the color version of this figure.

Schiller et al., 2015; Amsellem et al., 2017; Simon et al., 2017; Bermingham et al., 2018). There is disagreement, however, on whether enstatite chondrites also possess identical $^{44}Ca/^{40}Ca$ compositions to Earth. Some studies, e.g., Valdes et al. (2014) ($\delta^{44}Ca/^{40}Ca_{EL,EH}$ +0.90 to +1.01), Amsellem et al. (2017) ($\delta^{44}Ca/^{40}Ca_{EL,EH}$ +0.91 to +1.06), and Huang and Jacobsen (2017) ($\delta^{44}Ca/^{40}Ca_{EH}$ +0.90 to +0.96), reported no analytically resolvable Ca isotope fractionation between Earth and enstatite chondrites. In contrast, Simon and DePaolo (2010) reported that enstatite chondrites have $\delta^{44}Ca/^{40}Ca_{EH}$ compositions up to +0.5 higher than that of the Earth. The findings by Simon and DePaolo (2010) are also contrary to data for other multi-isotopic major elements, such as O (e.g., Clayton, 2003), Fe (e.g., Poitrasson et al., 2004; Craddock and Dauphas, 2011; Wang et al., 2014), Mg (e.g., Teng et al., 2010), and Si (e.g., Savage and Moynier, 2013), which indicate that enstatite chondrites and Earth are isotopically uniform.

4.3.1. The origin of mass-dependent Ca isotope variability between and within chondrite groups

It has been suggested that the variability between and within chondrite groups was established by a heterogeneous distribution of primitive solids with variable $\delta^{44}Ca/^{40}Ca$ compositions imparted during early disk processing (see Section 3) (Simon and DePaolo, 2010; Valdes et al., 2014; Huang and Jacobsen, 2017; Bermingham et al., 2018). For example, the light $\delta^{44}Ca/^{40}Ca$ signatures of bulk carbonaceous chondrites may reflect an overabundance of CAIs that are isotopically light as a result of non-equilibrium condensation (Simon and DePaolo, 2010) or ultrarefractory evaporative residue loss (Huang et al., 2012; Bermingham et al., 2018). Notably, however, CI chondrites do not contain obvious CAIs but do have light $\delta^{44}Ca/^{40}Ca$ signatures (Valdes et al., 2014; Huang and Jacobsen, 2017; Bermingham et al., 2018). Thus, the isotopically light Ca compositions of bulk carbonaceous chondrites cannot be exclusively attributed to CAI abundance, and likely reflects several generations of early nonequilibrium solid-gas fractionation including some prior to CAI formation (Simon and DePaolo, 2010). Neither can chondrules, which on average have $\delta^{44}Ca/^{40}Ca$ signatures identical to Earth, exclusively account for the light, variable $\delta^{44}Ca/^{40}Ca$ signatures in bulk carbonaceous chondrites.

As a fluid-mobile element, Ca can be strongly chemically fractionated among alteration products in chondrite matrices (Brearley, 2006); thus, it is possible that parent body alteration and/or post-fall terrestrial weathering produced mass-dependent Ca isotope fractionation effects in Ca-bearing chondrite phases. In this case, meteorites that variably sample phases modified by parent body alteration and/or terrestrial weathering may record isotopic differences between and within chondrite groups or conceal isotopic signatures initially imparted by the heterogeneous distribution of primitive solids.

Bermingham et al. (2018) suggested that if parent body aqueous alteration played a significant role in establishing $\delta^{44}Ca/^{40}Ca$ differences among chondrites, meteorites from chondrite groups that are substantially affected by low-temperature alteration (e.g., CI chondrites) would display greater $\delta^{44}Ca/^{40}Ca$ variability than those chondrite groups less affected (e.g., CO chondrites; Brearley, 2006). Indeed, CI chondrites ($\delta^{44}Ca/^{40}Ca_{CI}$ +0.42 to +1.13) show more Ca isotopic variation than CO chondrites ($\delta^{44}Ca/^{40}Ca_{CO}$ +0.77 to +1.19), thereby supporting the interpretation that parent body alteration plays a role in modifying the bulk $\delta^{44}Ca/^{40}Ca$ composition.

It is less clear if aqueous alteration as a result of terrestrial weathering has a measurable effect on the bulk $\delta^{44}Ca/^{40}Ca$ compositions of chondrites. Bermingham et al. (2018) noted that some oldhamite grains in MacAlpine Hills 88,136[13] display evidence of aqueous alteration (Lundberg et al., 1994), and suggested that alteration of oldhamite may have overprinted the primary Ca isotope signature imparted during accretion. Although a heterogeneous distribution of isotopically heavy oldhamite cannot be the sole cause of Ca isotopic variation in chondrite groups, it may engender Ca isotope variability within a group. Prior to this, it had been proposed that terrestrial alteration of oldhamite, which is highly soluble and easily aqueously mobilized, may result in its preferential dissolution and the removal of light Ca isotopes, resulting in an anomalously heavy oldhamite, and therefore bulk, $\delta^{44}Ca/^{40}Ca$ composition (Bermingham, 2011; Valdes et al., 2014). Valdes et al. (2014), however, dismissed this interpretation because the heavy $\delta^{44}Ca/^{40}Ca$ signatures for oldhamite obtained in their Indarch leaching experiment were not fractionated enough from the bulk composition to account for the magnitude of the MacAlpine Hills 88,136 offset from Earth as reported by Simon and DePaolo (2010). Conversely, according to the ab initio calculations of Huang et al. (2019), oldhamite should have lighter Ca isotope signatures compared to bulk under equilibrium conditions, which is in disagreement with the results of Valdes et al. (2014).

Further investigation of Ca isotopic variability in bulk samples as a consequence of fluid alteration of oldhamite (and other Ca-bearing phases) is necessary to constrain parent body compositions. As reported, bulk $\delta^{44}Ca/^{40}Ca$ data suggest that the Earth may have accreted

[13] MacAlpine Hills 88136 is the sample that provides the upper limit for the $\delta^{44}Ca/^{40}Ca$ + 0.5 offset of enstatite chondrites from Earth (Simon and DePaolo, 2010).

primarily from precursors with a composition similar to that of enstatite and/or ordinary chondrites. Future studies, however, should carefully evaluate for the effects of variably sampling isotopically heterogeneous primitive solids when using the Ca isotopic compositions of bulk meteorites to trace planetary building blocks.

4.4. Non-mass-dependent and mass-dependent Ca isotopic variation among achondrites, the Moon, and Mars

4.4.1. Achondrites

Mass-dependent and non-mass-dependent Ca isotopic data for bulk achondrites are presented in Figs. 4 and 5. Studies are in agreement that bulk angrites, aubrites, ureilites, winonaites, and presumed differentiation products of 4-Vesta (eucrites, diogenites) have $^{40}Ca/^{44}Ca$, $^{42}Ca/^{44}Ca$, $^{43}Ca/^{44}Ca$, and $^{46}Ca/^{44}Ca$ compositions that are indistinguishable from Earth at a precision of <0.2‰ (Simon and DePaolo, 2010; Valdes et al., 2014; Schiller et al., 2015; Schiller et al., 2018). These achondrite groups exhibit uniform non-mass-dependent $^{40}Ca/^{44}Ca$, $^{43}Ca/^{44}Ca$, and $^{46}Ca/^{44}Ca$ compositions that are not analytically resolved from Earth (Simon et al., 2009; Chen et al., 2011; Dauphas et al., 2014a; Schiller et al., 2015; Huang and Jacobsen, 2017; Yokoyama et al., 2017; Schiller et al., 2018). All primitive achondrite groups studied to date, however, have well-resolved ^{48}Ca deficits ($\varepsilon^{48}Ca/^{44}Ca$ −1 to −2) relative to Earth. Achondrite groups vary in degree of Ca isotope heterogeneity, with group-average ^{48}Ca deficits increasing in the order of eucrites > angrites > diogenites > ureilites (Chen et al., 2011; Dauphas et al., 2014a; Schiller et al., 2018).

The cause of $\varepsilon^{48}Ca/^{44}Ca$ heterogeneity is debated. In bulk achondrite groups, it may derive from variable mixing between material of Solar composition with isotopically anomalous material ejected from Type Ia or electron-capture supernova explosions (e.g., Simon et al., 2009; Moynier et al., 2010; Chen et al., 2011; Dauphas et al., 2014a; Huang and Jacobsen, 2017; Bermingham et al., 2018). Alternatively, $\varepsilon^{48}Ca/^{44}Ca$ anomalies may be indicative of selective and variable unmixing between two homogeneously distributed dust reservoirs via sublimation of thermally unstable, isotopically anomalous presolar carriers (Schiller et al., 2015). Regardless of the cause, it is evident that, despite unfractionated mass-dependent Ca isotopic compositions of bulk achondrites from that of Earth, planetary formation and differentiation processes were ineffective in fully homogenizing the Ca isotopic composition of the Solar System.

4.4.2. The Earth-Moon system

The canonical giant impact theory for the formation of the Moon proposes that a Mars-sized body (Theia) collided with the proto-Earth and ejected material into an Earth-orbiting disk, which subsequently re-accreted to form the Moon (e.g., Hartmann and Davis, 1975; Cameron and Ward, 1976). A long-standing question concerns the composition of the impactor. Early impact models predicted the Moon to be largely derived from the impactor (e.g., Cameron, 2000; Canup and Asphaug, 2001, Canup, 2012); however, in this scenario it is remarkable that the O, Si, Ti, Mg, and Cr isotopic compositions of Earth and the Moon are indistinguishable within analytical uncertainty (e.g., Lugmair and Shukolyukov, 1998; Wiechert et al., 2001; Spicuzza et al., 2007; Fitoussi et al., 2010; Qin et al., 2010; Armytage et al., 2012; Warren, 2011; Zhang et al., 2012; Sedaghatpour et al., 2013; Young et al., 2016; Bonnand et al., 2016; Mougel et al., 2017). Given the variability exhibited by these isotopes among other planetary bodies, the similarity between the Earth and the Moon is significant. This similarity has been used to support the interpretation that the proto-Earth and the impactor formed from the same reservoir of material located in the inner part (≤1.5 AU) of the disk (Jacobsen et al., 2013; Dauphas et al., 2014b), or that the Moon was primarily formed from the proto-Earth (Zhang et al., 2012). Alternatively, the proto-Earth and the impactor may have been compositionally distinct, but this would require, for example, turbulent mixing and equilibration in the aftermath of the giant impact to isotopically homogenize the system (Pahlevan and Stevenson, 2007; Young et al., 2016). Recently, numerical calculations based on a fast-spinning Earth and a high energy impact (Ćuk and Stewart, 2012; Lock et al., 2018) have predicted isotopic similarity between the Earth and Moon as a consequence of the Moon's direct condensation from a homogenized disk of vapor deriving primarily from Earth's mantle (Lock et al., 2018; see recent review by Lock et al., 2020).

The number of studies that have published Ca isotopic data for bulk lunar samples is still limited (Figs. 4 and 5), but the few available data show that the Moon and Earth have identical mass-dependent and non-mass-dependent Ca isotopic compositions. In 15 lunar basalts (meteoritic, as well as from Apollo 11, 12, 14, and 15), Simon and DePaolo (2010), Valdes et al. (2014), and Simon et al. (2017) found $\delta^{44}Ca/^{40}Ca$ compositions indistinguishable from Earth. There is no systematic variation in Ca isotopic composition between brecciated and unbrecciated basalts, nor between high-Ti (Apollo 11) and low-Ti (Apollo 12, 14, 15) basalts. Three green glass samples exhibit no resolvable fractionation from lunar basalts and Earth. One anorthosite, however, Dhofar 026, is isotopically light relative to Earth (Schiller et al., 2018).

Non-mass-dependent Ca isotopic data has only been reported for four basaltic meteorites and one Apollo 16 anorthosite. Neither the $^{48}Ca/^{44}Ca$ compositions measured in basalts (Schiller et al., 2018) nor the $^{40}Ca/^{44}Ca$, $^{43}Ca/^{44}Ca$ and $^{48}Ca/^{44}Ca$ compositions measured in the anorthosite show any fractionation from Earth within analytical uncertainty.

What the Ca isotopic similarity between the Earth and Moon indicates about their genetic relationship is still not clear. It is yet to be understood if the data best support (i) the formation of the Moon predominantly from proto-Earth material (Zhang et al., 2012), (ii) the isotopic equilibration of the Earth-Moon system after the giant impact (Pahlevan and Stevenson, 2007; Young et al., 2016), or (iii) the derivation of the proto-Earth and the impactor from the same, isotopically homogeneous reservoir of material (Jacobsen et al., 2013; Dauphas et al., 2014b). Thus, the Earth and Moon's identical Ca isotopic signatures remain a significant characteristic of the system that dynamical models need to reproduce.

4.4.3. Mars

Twelve Martian samples have been analyzed for non-mass-dependent Ca isotopic compositions. Five samples do not exhibit distinct non-mass-dependent $^{40}Ca/^{44}Ca$, $^{43}Ca/^{44}Ca$, or $^{46}Ca/^{44}Ca$ compared to Earth (Simon et al., 2009; Chen et al., 2011) (Fig. 4). The two exceptions, ALH84001 and QUE9420, have slightly elevated $\varepsilon^{40}Ca/^{44}Ca$ compositions (+0.59 and +0.88, respectively). These small excesses are likely not a primary feature, but rather may be attributed to an unrecognized secondary alteration process on Mars (Simon et al., 2009). Additionally, Chen et al. (2011) and Schiller et al. (2018) measured the $\varepsilon^{40}Ca/^{44}Ca$ compositions of nine Martian meteorites. While Chen et al. (2011) did not detect any significant departures of Martian meteorites from Earth, Schiller et al. (2018), who measured at slightly higher precision, found that they exhibit an average resolvable $\varepsilon^{40}Ca/^{44}Ca$ deficit of -0.2 ± 0.03 compared to Earth.

Comparatively more samples have been analyzed for mass-dependent Ca isotopic compositions (Fig. 5). Magna et al. (2015) performed the most comprehensive study to date by measuring the mass-dependent Ca isotopic composition of 22 different shergottites, nakhlites, chassignites (SNCs), and a Martian OPX (ALH84001), and demonstrated that the average $\delta^{44}Ca/^{40}Ca$ of Martian meteorites is indistinguishable from Earth, ordinary chondrites, and enstatite chondrites, within analytical uncertainty. Likewise, Simon and DePaolo (2010) did not identify $\delta^{44}Ca/^{40}Ca$ variation in a shergottite and ALH94001. Combining the datasets from Magna et al. (2015) and Simon and DePaolo (2010), Martian meteorites exhibit a range in $\delta^{44}Ca/^{40}Ca$ of ~ +0.4‰ (from $\delta^{44}Ca/^{40}Ca$ +0.71 to +1.15) and may reflect mass-dependent Ca isotopic fractionation during magmatic differentiation, though this has not been explored in detail. Magna et al. (2015)

estimated a mean $\delta^{44}Ca/^{40}Ca$ of +1.04 ± 0.09 for bulk silicate Mars, identical to the estimate for BSE by Kang et al. (2017), which is consistent with the assertion made by Simon and DePaolo (2010) of uniform bulk Ca isotopic compositions of the inner Solar System planets. The similarity in $\delta^{44}Ca/^{40}Ca$ between Mars and the Earth can be interpreted to indicate that isotopic homogenization for Ca was complete by the time the inner Solar System planets formed (Simon et al., 2009).

As with Earth, there is a general consensus that Mars accreted from a mixture of materials represented by known meteorite types. Given that the estimated $\delta^{44}Ca/^{40}Ca$ composition of bulk silicate Mars overlaps with those of ordinary chondrites, enstatite chondrites, some carbonaceous chondrite types, and most achondrites, the constraints that mass-dependent Ca isotopic data place on the building blocks of Mars are limited. Nevertheless, a variety of models have been proposed. Most attempts to model combinations of precursor material types based on stable isotope constraints agree that the likely building blocks of Mars were predominantly non-carbonaceous (Lodders and Fegley, 1997; Sanloup et al., 1999; Mohapatra and Murty, 2003; Burbine and O'Brien, 2004; Tang and Dauphas, 2014; Fitoussi et al., 2016; Liebske and Khan, 2019). There is disagreement, however, in the relative proportions of precursor types. For example, Lodders and Fegley calculated that Mars could be made of 85% ordinary chondrites + 11% CV chondrites + 4% CI chondrites. In contrast, the results of the model from Sanloup et al. (1999) point to an exclusively non-carbonaceous Mars, made up of 55% H chondrites + 45% enstatite chondrites. This was subsequently supported by the results of Tang and Dauphas (2014). Dauphas et al. (2014a) calculated $\varepsilon^{48}Ca/^{40}Ca$ compositions for bulk Mars using the mixtures proposed by Lodders and Fegley (1997) and Sanloup et al. (1999) and found that only the value produced by assuming the mixture of Sanloup et al. (1999) (−0.24 ± 0.30) agrees with the average $\varepsilon^{48}Ca/^{40}Ca$ composition for SNCs measured by Chen et al. (2011) (−0.11 ± 0.16). However, neither the Lodders and Fegley (1997) nor Sanloup et al. (1999) models, nor any in the studies mentioned above, are able to self-consistently explain isotopic data, major element chemistry, and geophysical properties simultaneously.

5. Future directions

The versatility of the Ca isotope system allows it to be used to address key issues in cosmochemistry, including: (1) the combination and timing of stellar precursors into the Solar nebula, (2) the significance of non-mass-dependent isotopic compositions of refractory inclusions regarding mixing processes and location of these reservoirs in the disk, and (3) the link between non-mass-dependent and mass-dependent isotopic compositions. The field of Ca isotope cosmochemistry is rapidly expanding as new research pathways emerge.

A promising avenue of research is to assess which (and to what extent) nebular processes fractionate Ca isotopes. This could be advanced by obtaining coupled mass-dependent and non-mass-dependent Ca isotopic data on disk condensates. This dataset would identify if the thermal events that caused non-mass-dependent Ca isotope anomalies were linked to events that generated mass-dependent Ca isotope fractionation (e.g., Niederer and Papanastassiou, 1984; Huang et al., 2012; Simon et al., 2017; Bermingham et al., 2018).

Another research pathway is investigating how Ca isotopes fractionate in response to parent body and terrestrial aqueous alteration processes. On parent bodies, multi-stage, low-temperature aqueous events mobilized and redistributed elements within the matrix and between individual components and the matrix (e.g., McGuire and Hashimoto, 1989; Kojima and Tomeoka, 1996; Krot et al., 2000b; McSween Jr., 1987; Brearley, 2006). As Ca is fluid mobile, it is potentially sensitive to isotopic fractionation effects as a result of elemental redistribution among primary phases and/or the formation of secondary phases. Post-fall terrestrial weathering may also have resulted in Ca isotope fractionation, depending on the residence time and location of the meteorite (e.g., Gounelle and Zolensky, 2001; Bland et al., 2006). Presently, there exists only indirect or presumed evidence of Ca isotopic fractionation in meteorites as a result of aqueous alteration on the bulk scale (e.g., Magna et al., 2015; Deng et al., 2018; Bermingham et al., 2018) and on the component scale (e.g., Bermingham et al., 2018). An important research focus for the near future is to identify potential mass-dependent Ca isotopic effects of parent body and terrestrial aqueous alteration events on bulk meteorites and their components. Determining the extent to which these effects obscure primary mass-dependent Ca isotopic variability is required to identify planetary building blocks (Simon and DePaolo, 2010; Valdes et al., 2014; Simon et al., 2017; Bermingham et al., 2018).

Future studies that concurrently collect mass-dependent and non-mass-dependent Ca isotopic data in component and bulk samples will be most informative in addressing the significance of anomalous Ca isotopic compositions in chondrite components regarding mixing processes and the location of parent body reservoirs in the disk. The use of multi-isotopic proxies of elements that record thermal processing events (e.g., REE, O, Al, Mg, and Ti), along with Ca, will be particularly useful for providing constraints on the physical conditions of different parts of the protoplanetary disk (Bermingham et al., 2018). Forthcoming work should continue to take advantage of the extensive datasets that have made Ca isotopes a benchmark for comparison with other isotope systems. This approach is required if a comprehensive, self-consistent formation model of the Solar System is to be formulated using isotopic datasets derived from meteorites and their components.

To this end, future work would benefit from refining current high-precision isotope measurement techniques for bulk rocks and components and coupling them with petrographic observations, mineral compositional data, major and trace element data, and in situ analytical and imaging techniques. This work could include advancing established analytical techniques (e.g., SIMS, NanoSIMS, and LA-MC-ICP-MS), or employing new ones such as atom probe tomography (APT), which is increasingly being used in geo- and cosmochemistry to determine isotopic compositions and spatial distributions in three dimensions at the nanometer level (e.g., Heck et al., 2014; Greer et al., 2020). Future studies may also consider using advanced micromilling techniques (following Simon et al., 2017) to completely remove components and their rims for ex situ work.

Finally, we emphasize the importance of standardizing future Ca isotopic data reporting methods. A significant problem in the Ca isotope community is that the direct comparison of published datasets is hindered by the lack of universal agreement on which reference material should be used as the standard for Ca isotopes. Consequently, over the years Ca isotopic data have been reported relative to many different reference materials (e.g., SRM915a, SRM915b, CaF_2, modern seawater, and BSE). This is further complicated by the fact that mass-dependent Ca isotope studies are inconsistent in which isotope ratios they report. Some report, for example, deviations in $^{44}Ca/^{40}Ca$, $^{40}Ca/^{44}Ca$, $^{44}Ca/^{42}Ca$, or $^{42}Ca/^{44}Ca$, while others report data as F_{Ca} ($\delta^{40}Ca/^{44}Ca$ or $\delta^{44}Ca/^{40}Ca$ in ‰/amu). For non-mass-dependent data, many studies are unclear about or make no mention of which isotope ratio and mass fractionation law are used to normalize and correct for instrumental mass bias. In order to limit unnecessary complexity in the comparison of cosmochemical Ca isotopic datasets, we encourage more uniformity in data reporting. Specifically, we recommend the presentation of mass-dependent variations in the form of $\delta^{44}Ca/^{40}Ca$ and the conversion of data to the SRM915a scale, regardless of original reference material, to facilitate interlaboratory comparison. For non-mass-dependent data, we propose that data are normalized to the terrestrial $^{42}Ca/^{44}Ca$ composition relative to CaF_2 as defined by Russell et al. (1978) using the appropriate mass fractionation law for the study.

6. Conclusions

The chemical properties of Ca make its isotopes among the most robust tracers of cosmochemical processes. Here, mass-dependent and

non-mass-dependent Ca isotopic variations among bulk meteorites and their components have been explored in the context of tracing the establishment and preservation of non-mass-dependent heterogeneities in the disk, understanding the effects of nebular thermal processing, and constraining the compositions of planetary building blocks.

Resolved non-mass-dependent isotope effects, generally considered to be the result of a poorly homogenized protoplanetary disk, are present in both bulk chondrites and their components. It is clear from these variations that isotopically distinct contributions of various nucleosynthetic origins were incorporated into the disk and survived long enough to be preserved in planet-building materials. Debate, however, persists as to how and when the presolar grain carriers of these Ca isotope anomalies became heterogeneously distributed in the disk. Presently, non-mass-dependent Ca isotope anomalies in most chondrite components are decoupled from mass-dependent variations. This suggests the thermal processing events that generated Ca isotope anomalies occurred at a different time or location in the protoplanetary disk from those that generated mass-dependent Ca isotope fractionations.

Compared to chondrite components, bulk meteorites display limited, but resolved, mass-dependent and non-mass-dependent Ca isotope variations. In the context of chondritic Earth models, these variations provide constraints on the genetic links between chondrites and Earth, as well as between Earth and the Moon. Specifically, Ca isotopic data support the interpretation that 1) material isotopically similar to ordinary or enstatite chondrites comprised a significant portion of the precursors that accreted to Earth, and 2) the Moon may have formed predominantly from proto-Earth material, or, if from impactor material, then only if the impactor had the same isotopic composition as the proto-Earth or if the vaporous material from both fully homogenized after impact. These interpretations, however, rely on the assumption that bulk samples are representative of parent body compositions. Determining the extent to which parent body and terrestrial alteration effects modify primary mass-dependent Ca isotope variability is critical to constraining the nature of planetary building blocks.

Declaration of Competing Interest

The authors certify that they have no conflicts of interest to declare. All co-authors have seen and agree with the contents of the manuscript and there is no financial interest to report. We certify that the submission is original work and is not under review at any other publication.

Acknowledgements

The authors would like to thank editor Don Porcelli and special issue editors Matt Fantle and Liz Griffith for their guidance. We would like to thank two anonymous reviewers for their comments. We are grateful to Andy Davis for his insightful comments which improved the manuscript, Nikolaus Gussone for assistance with $\delta^{44}Ca/^{40}Ca$ conversions between different standards, and Hamed Pourkhorsandi and François Tissot for constructive discussions. M.C.V. was supported by the Fondation Wiener-Anspach Postdoctoral Fellowship at the University of Cambridge and the John Caldwell Meeker Postdoctoral Fellowship through the Negaunee Integrative Research Center's Robert A. Pritzer Center for Meteoritics and Polar Studies at the Field Museum. K.R.B. received support from NASA Emerging Worlds grants 80NSSC18K0496 and NNX16AN07G, NASA SSERVI grant NNA14AB07A, and the Department of Earth and Planetary Sciences, Rutgers University. S.H. was supported by NSF grant AST-1910955. J.I.S. was supported by NASA Planetary Science Division, Solar System Workings, and Emerging Worlds Programs.

Appendix A. Supplementary data

Supplementary data to this article can be found online at https://doi.org/10.1016/j.chemgeo.2021.120396.

References

Akram, W., Schönbächler, M., Bisterzo, S., Gallino, R., 2015. Zirconium isotope evidence for the heterogeneous distribution of s-process materials in the Solar System. Geochim. Cosmochim. Acta 165, 484–500.
Alexander, C.M., Grossman, J.N., Ebel, D.S., Ciesla, F.J., 2008. The formation conditions of chondrules and chondrites. Science 320, 1617–1619.
Allègre, C.J., Poirier, J.-P., Humler, E., Hofmann, A.W., 1995. The chemical composition of the Earth. Earth Planet. Sci. Lett. 134, 515–526.
Allen, J.M., Grossman, L., Lee, T., Wasserburg, G.J., 1979. Mineralogical study of an isotopically-unusual Allende inclusion. Lunar Planet. Sci. 10, 24–26.
Allen, J.M., Grossman, L., Lee, T., Wasserburg, G.J., 1980. Mineralogy and petrography of HAL, an isotopically-unusual Allende inclusion. Geochim. Cosmochim. Acta 44, 685–699.
Amari, S., Anders, E., Virag, A., Zinner, E., 1990. Interstellar graphite in meteorites. Nature 345, 238–240.
Amos, S., Gross, J.L., Thoennessen, M., 2011. Discovery of the calcium, indium, tin, and platinum isotopes. At. Data Nucl. Data Tables 97, 383–402.
Amsellem, E., Moynier, F., Pringle, E.A., Bouvier, A., Chen, H., Day, J.M.D., 2017. Testing the chondrule-rich accretion model for planetary embryos using calcium isotopes. Earth Planet. Sci. Lett. 469, 75–83.
Amsellem, E., Moynier, F., Puchtel, I.S., 2019. Evolution of the Ca isotopic composition of the mantle. Geochim. Cosmochim. Acta 258, 195–206.
Anders, E., 1971. How well do we know "cosmic" abundances? Geochim. Cosmochim. Acta 35, 516–522.
Anders, E., Grevesse, N., 1989. Abundances of the elements: meteoritic and Solar. Geochim. Cosmochim. Acta 53, 197–214.
Antonelli, M.A., Simon, J.I., 2020. Calcium isotopes in high-temperature terrestrial processes. Chem. Geol. 548, 119651.
Armytage, R.M.G., Georg, R.B., Williams, H.M., Halliday, A.N., 2012. Silicon isotopes in lunar rocks: implications for the Moon's formation and the early history of the Earth. Geochim. Cosmochim. Acta 77, 504–514.
Bermingham, K.R., 2011. Stable Ba and Ca Isotope Compositions of Meteorites and their Components: Insights into the Early Solar System. PhD thesis. Westfälische Wilhelms-Universität, pp. 98–102.
Bermingham, K.R., Mezger, K., Scherer, E.E., Horan, M.F., Carlson, R.W., Upadhyay, D., Magna, T., Pack, A., 2016. Barium isotope abundances in meteorites and their implications for early Solar System evolution. Geochim. Cosmochim. Acta 175, 282–298.
Bermingham, K.R., Füri, E., Lodders, K., Marty, B., 2020. The NC-CC isotope dichotomy: Implications for the chemical and isotopic evolution of the early Solar System. Space Sci. Rev. 216 (133).
Bermingham, K.R., Gussone, N., Mezger, K., Krause, J., 2018. Origins of mass-dependent and mass-independent Ca isotope variations in meteoritic components and meteorites. Geochim. Cosmochim. Acta 226, 206–223.
Bermingham, K.R., Walker, R.J., 2017. The ruthenium isotopic composition of the oceanic mantle. Earth Planet. Sci. Lett. 474, 466–473.
Bernatowicz, T., Fraundorf, G., Tang, M., Anders, E., Wopenka, B., Zinner, E., Fraundorf, P., 1987. Evidence for interstellar SiC in the Murray carbonaceous meteorite. Nature 330, 24–31.
Binzel, R.P., 1996. Searching for resolution in the S-asteroid/ordinary chondrite debate. Meteorit. Planet. Sci. 31, 165.
Bischoff, A., Keil, K., 1984. Al-rich objects in ordinary chondrites: related origin of carbonaceous and ordinary chondrites and their constituents. Geochim. Cosmochim. Acta 48, 693–709.
Bischoff, A., Vogel, N., Roszjar, J., 2011. The Rumuruti chondrite group. Chem. Erde/Geochemistry 71, 101–133.
Black, D.C., Pepin, R.O., 1969. Trapped neon in meteorites II. Earth Planet. Sci. Lett. 6, 395–405.
Bland, P.A., Alard, O., Benedix, G.K., Kearsley, A.T., Menzies, O.N., Watt, L.E., Rogers, N. W., 2005. Volatile fractionation in the early Solar System and chondrule/matrix complementarity. Proc. Natl. Acad. Sci. 102, 13755–13760.
Bland, P.A., Zolensky, M.E., Benedix, G.K., Sephton, M.A., 2006. Weathering of chondritic meteorites. In: Lauretta, D.S., McSween Jr., H.Y. (Eds.), Meteorites and the early Solar System II. University of Arizona Press, pp. 853–867.
Bogard, D.D., Nyquist, L.E., Bansal, B.M., Garrison, D.H., Wiesmann, H., Herzog, G.F., Albrecht, A.A., Vogt, S., Klein, J., 1995. Neutron-capture ^{36}Cl, ^{41}Ca, ^{36}Ar, and ^{150}Sm in large chondrites: evidence for high fluences of thermalized neutrons. J. Geophys. Res. 100, 9401–9416.
Bonnand, P., Parkinson, I.J., Anand, M., 2016. Mass dependent fractionation of stable chromium isotopes in mare basalts: implications for the formation and the differentiation of the Moon. Geochim. Cosmochim. Acta 175, 208–221.
Boss, A.P., 1995. Collapse and fragmentation of molecular cloud cores. II. Collapse induced by stellar shock waves. Astrophys. J. 439, 224–236.
Bottke, W.F., Nesvorný, D., Grimm, R.E., Morbidelli, A., O'Brien, D.P., 2006. Iron meteorites as remnants of planetesimals formed in the terrestrial planet region. Nature 439, 821–824.
Boynton, W.V., 1975. Fractionation in the Solar nebula: condensation of yttrium and the rare earth elements. Geochim. Cosmochim. Acta 39, 569–584.
Brearley, A.J., 2006. The action of water. In: Lauretta, D.S., McSween Jr., H.Y. (Eds.), Meteorites and the Early Solar System II. University of Arizona Press, pp. 587–624.
Brearley, A.J., Jones, R.H., 1998. Chondritic meteorites. In: Papike, J.J. (Ed.), Planetary Materials, Reviews in Mineralogy, 36. Mineralogical Society of America, 3.1–3.398.
Bullock, E.S., Knight, K.B., Richter, F.M., Kita, N.T., Ushikubo, T., MacPherson, G.J., Davis, A.M., Mendybaev, R.A., 2013. Mg and Si isotopic fractionation patterns in

types B1 and B2 CAIs: implications for formation under different nebular conditions. Meteorit. Planet. Sci. 48, 1440–1458.
Burbidge, E.M., Burbidge, G.R., Fowler, W.A., Hoyle, F., 1957. Synthesis of the elements in stars. Rev. Mod. Phys. 29, 547–650.
Burbine, T.H., O'Brien, K.M., 2004. Determining the possible building blocks of the Earth and Mars. Meteorit. Planet. Sci. 39, 667–668.
Cameron, A.G.W., 1957. Stellar Evolution, Nuclear Astrophysics, and Nucleogenesis. Chalk River Report, CLR-41. Chalk River, Ontario, pp. 1–197.
Cameron, A.G.W., 1962. The formation of the Sun and planets. Icarus 1, 13–69.
Cameron, A.G.W., 2000. Higher resolution simulations of the Giant Impact. In: Canup, R. M., Righter, K. (Eds.), Origin of the Earth and Moon. University of Arizona Press, pp. 133–144.
Cameron, A.G.W., Truran, W., 1977. The supernova trigger for formation of the Solar System. Icarus 30, 447–461.
Cameron, A.G.W., Ward, W.R., 1976. The origin of the Moon. Lunar Sci. 7, 120–122.
Canup, R.M., 2012. Forming a Moon with an Earth-like composition via a giant impact. Science. 338, 1052–1055.
Canup, R.M., Asphaug, E., 2001. Origin of the Moon in a giant impact near the end of the Earth's formation. Nature 412, 708–712.
Chambers, J.E., 2001. Making more terrestrial planets. Icarus 152, 205–224.
Chen, H.-W., Lee, T., Lee, D.-C., Shen, J.J.-S., Chen, J.-C., 2011. ^{48}Ca heterogeneity in differentiated meteorites. Astrophys. J. 743, L23.
Chen, H.-W., Lee, T., Lee, D.-C., Chen, J.-C., 2015. Correlation of ^{48}Ca, ^{50}Ti, and ^{138}La heterogeneity in the Allende refractory inclusions. Astrophys. J. 806. L21.
Clayton, R.N., 2002. Self-shielding in the Solar nebula. Nature 415, 860–861.
Clayton, R.M., 2003. Oxygen Isotopes in the Solar System. Space Sci. Rev. 106, 19–32.
Clayton, R.N., 2004. Oxygen isotopes in meteorites. In: Davis, A.M. (Ed.), Meteorites, Planets, and Comets. Elsevier, Oxford, pp. 129–142. Vol. 1 Treatise on Geochemistry (Eds. Holland, H. D. and Turekian, K. K.).
Clayton, R.N., Grossman, L., Mayeda, T.K., 1973. A component of primitive nuclear composition in carbonaceous meteorites. Science 182, 485–488.
Connelly, J.N., Bizzarro, M., Krot, A.N., Nordlund, Å., Wielandt, D., Ivanova, M.A., 2012. The absolute chronology and thermal processing of solids in the Solar protoplanetary disk. Science 338, 651.
Craddock, P.R., Dauphas, N., 2011. Iron isotopic compositions of geological reference materials and chondrites. Geostand. Geoanal. Res. 35, 101–123.
Ćuk, M., Stewart, S.T., 2012. Making the Moon from a fast-spinning Earth: a giant impact followed by resonant despinning. Science 338, 1047–1052.
Cuzzi, J.N., Alexander, C.M.O., 2006. Chondrule formation in particle- rich nebular regions at least hundreds of kilometres across. Nature 441, 483–485.
Dauphas, N., 2017. The isotopic nature of the Earth's accreting material through time. Nature 541, 521–524.
Dauphas, N., Remusat, L., Chen, J.H., Roskosz, M., Papanastassiou, D.A., Stodolna, J., Guan, Y., Ma, C., Eiler, J.M., 2010. Neutron-rich chromium isotope anomalies in supernova nanoparticles. Astrophys. J. 720, 1577–1591.
Dauphas, N., Chen, J.H., Zhang, J., Papanastassiou, D.A., Davis, A.M., Travaglio, C., 2014a. Calcium-48 isotopic anomalies in bulk chondrites and achondrites: evidence for a uniform isotopic reservoir in the inner protoplanetary disk. Earth Planet. Sci. Lett. 407, 96–108.
Dauphas, N., Burkhardt, C., Warren, P.H., Teng, F.-Z., 2014b. Geochemical arguments for an Earth-like Moon-forming impactor. Philos. Trans. R. Soc. A 372, 20130244.
Davis, A.M., Grossman, L., 1979. Condensation and fractionation of rare earths in the Solar nebula. Geochim. Cosmochim. Acta 43, 1611–1632.
Davis, A.M., Tanaka, T., Grossman, L., Lee, T., Wasserburg, G.J., 1982. Chemical composition of HAL, an isotopically-unusual Allende inclusion. Geochim. Cosmochim. Acta 46, 1627–1651.
Davis, A.M., Hashimoto, A., Clayton, R.N., Mayeda, T.K., 1990. Isotope mass fractionation during evaporation of Mg_2SiO_4. Nature 347, 655–658.
Davis, A.M., Richter, F.M., Mendybaev, R.A., Janney, P.E., Wadhwa, M., McKeegan, K.D., 2015. Isotopic mass fractionation laws for magnesium and their effects on ^{26}Al–^{26}Mg systematics in Solar system materials. Geochim. Cosmochim. Acta 158, 245–261.
Davis, A.M., Zhang, J., Greber, N.D., Hu, J., Tissot, F.L.H., Dauphas, N., 2018. Titanium isotopes and rare earth patterns in CAIs: evidence for thermal processing and gas-dust decoupling in the protoplanetary disk. Geochim. Cosmochim. Acta 221, 275–295.
Deng, Z., Moynier, F., van Zuilen, K., Sossi, P.A., Pringle, E.A., Chaussidon, M., 2018. Lack of resolvable titanium stable isotopic variations in bulk chondrites. Geochim. Cosmochim. Acta 239, 409–419.
Drake, M.J., Righter, K., 2002. Determining the composition of the Earth. Nature 416, 39–44.
Esat, T.M., Spear, R.H., Taylor, S.R., 1986. Isotope anomalies induced in laboratory distillation. Nature 319, 576–578.
Fahey, A., Goswami, J.N., McKeegan, K.D., Zinner, E., 1987a. ^{26}Al, ^{244}Pu, ^{50}Ti, REE, and trace element abundances in hibonite grains from CM and CV meteorites. Geochim. Cosmochim. Acta 51, 329–350.
Fahey, A.J., Goswami, J.N., McKeegan, K.D., Zinner, E., 1987b. ^{16}O excesses in Murchison and Murray hibonites: a case against a late supernova injection origin of isotopic anomalies in O, Mg, Ca, and Ti. Astrophys. J. 323, L91–L95.
Fantle, M.S., Tipper, E.T., 2014. Calcium isotopes in the global biogeochemical Ca cycle: implications for development of a Ca isotope proxy. Earth Sci. Rev. 129, 148–177.
Fischer-Gödde, M., Burkhardt, C., Kruijer, T.S., Kleine, T., 2015. Ru isotope heterogeneity in the Solar protoplanetary disk. Geochim. Cosmochim. Acta 168, 151–171.
Fitoussi, C., Bourdon, B., Pahlevan, K., Wieler, R., 2010. Si isotope constraints on the moon-forming impact. Lunar Planet. Sci. 41. #1533.
Fitoussi, C., Bourdon, B., Wang, X., 2016. The building blocks of Earth and Mars: a close genetic link. Earth Planet. Sci. Lett. 434, 151–160.
Galy, A., Young, E.D., Ash, R.D., O'Nions, R.K., 2000. The formation of chondrules at high gas pressures in the Solar nebula. Science 290, 1751–1754.
Goswami, J.N., 2004. Short-lived nuclides in the early Solar System: the stellar connection. New Astron. Rev. 48, 125–132.
Gounelle, M., Zolensky, M.E., 2001. A terrestrial origin for sulfate veins in CI1 chondrites. Meteorit. Planet. Sci. 36, 1321–1329.
Gradie, J.C., Tedesco, E.F., 1982. Compositional structure of the asteroid belt. Science 216, 1405–1407.
Greer, J., Rout, S.S., Isheim, D., Seidman, D.N., Wieler, R., Heck, P.R., 2020. Atom probe tomography of space-weathered lunar ilmenite grain surfaces. Meteorit. Planet. Sci. 55, 426–440.
Grewal, D.S., Dasgupta, R., Sun, C., Tsuno, K., Costin, G., 2019. Delivery of carbon, nitrogen, and sulfur to the silicate Earth by a giant impact. Sci. Adv. 5, 1–12.
Grimm, R.E., McSween Jr., H.Y., 1993. Heliocentric zoning of the asteroid belt by aluminum-26 heating. Science 259, 653–655.
Grossman, L., 1972. Condensation in the primitive Solar nebula. Geochim. Cosmochim. Acta 36, 597–619.
Grossman, L., Steele, I., 1976. Amoeboid olivine aggregates in the Allende meteorite. Geochim. Cosmochim. Acta 40, 149–155.
Grossman, L., Ebel, D.S., Simon, S.B., Davis, A.M., Richter, F.M., Parsad, N.M., 2000. Major element chemical and isotopic compositions of refractory inclusions in C3 chondrites: the separate roles of condensation and evaporation. Geochim. Cosmochim. Acta 64, 2879–2894.
Hartmann, W.K., Davis, D.R., 1975. Satellite-sized planetesimals and lunar origin. Icarus 24, 504–514.
He, Y., Wang, Y., Zhu, C., Huang, S., Li, S., 2017. Mass-independent and mass dependent Ca isotopic compositions of thirteen geological standards measured by thermal ionization mass spectrometry. Geostand. Geoanal. Res. 41, 283–302.
Heck, P.R., Stadermann, F.J., Isheim, D., Auciello, O., Daulton, T.L., Davis, A.M., Elam, J. W., Floss, C., Hiller, J., Larson, D.J., Lewis, J.B., Mane, A., Pellin, M.J., Savina, M.R., Seidman, D.N., Stephan, T., 2014. Atom-probe analyses of nanodiamonds from Allende. Meteorit. Planet. Sci. 49, 453–467.
Heck, P.R., Greer, J., Kööp, L., Trappitsch, R., Gyngard, F., Busemann, H., Maden, C., Ávila, J.N., Davis, A.M., Wieler, R., 2020. Lifetimes of interstellar dust from cosmic ray exposure ages of presolar silicon carbide. Proc. Natl. Acad. Sci. 1107, 1884–1889.
Hinton, R.W., Bischoff, A., 1984. Ion microprobe magnesium isotope analysis of plagioclase and hibonite from ordinary chondrites. Nature 308, 169–172.
Hinton, R.W., Davis, A.M., Scatena-Wachel, D.E., Grossman, L., Draus, R.J., 1988. A chemical and isotopic study of hibonite-rich refractory inclusions in primitive meteorites. Geochim. Cosmochim. Acta 52, 2573–2598.
Huang, S., Jacobsen, S.B., 2017. Calcium isotopic compositions of chondrites. Geochim. Cosmochim. Acta 201, 364–376.
Huang, S., Farkas, J., Jacobsen, S.B., 2010. Calcium isotopic fractionation between clinopyroxene and orthopyroxene from mantle peridotites. Earth Planet. Sci. Lett. 292, 337–344.
Huang, S., Farkas, J., Yu, G., Petaev, M.I., Jacobsen, S.B., 2012. Calcium isotopic ratios and rare earth element abundances in refractory inclusions from the Allende CV3 chondrite. Geochim. Cosmochim. Acta 77, 252–265.
Huang, F., Zhou, C., Wang, W., Kang, J., Wu, Z., 2019. First-principles calculations of equilibrium Ca isotope fractionation: Implications for oldhamite formation and evolution of lunar magma ocean. Earth Planet. Sci. Lett. 510, 153–160.
Humayun, M., Cassen, P., 2000. Processes determining the volatile abundances of the meteorites and terrestrial planets. In: Canup, R.M., Righter, K. (Eds.), Origin of the Earth and Moon. University of Arizona Press, pp. 3–24.
Ireland, T.R., 1988. Correlated morphological, chemical, and isotopic characteristics of hibonites from the Murchison carbonaceous chondrite. Geochim. Cosmochim. Acta 52, 2827–2839.
Ireland, T.R., 1990. PreSolar isotopic and chemical signatures in hibonite-bearing refractory inclusions from the Murchison carbonaceous chondrite. Geochim. Cosmochim. Acta 54, 3219–3237.
Ireland, T.R., Compston, W., 1987. Large heterogeneous ^{26}Mg excesses in a hibonite from the Murchison meteorite. Nature 327, 689–692.
Ireland, T.R., Fahey, A.J., Zinner, E.K., 1989. Isotopic and chemical constraints on the formation of HAL-type refractory inclusions. Lunar Planet. Sci. 20, 442–443.
Ireland, T.R., Fahey, A.J., Zinner, E.K., 1991. Hibonite-bearing microspherules: a new type of refractory inclusions with large isotopic anomalies. Geochim. Cosmochim. Acta 55, 367–379.
Ireland, T.R., Zinner, E.K., Fahey, A.J., Esat, T.M., 1992. Evidence for distillation in the formation of HAL and related hibonite inclusions. Geochim. Cosmochim. Acta 56, 2503–2520.
Jacobsen, B., Yin, Q.-Z., Moynier, F., Amelin, Y., Krot, A.N., Nagashima, K., Hutcheon, I. D., Palme, H., 2008. ^{26}Al–^{26}Mg and ^{207}Pb–^{206}Pb systematics of Allende CAIs: canonical Solar initial ^{26}Al/^{27}Al ratio reinstated. Earth Planet. Sci. Lett. 272, 353–364.
Jacobsen, S.B., Petaev, M., Huang, S., Sasselov, D., 2013. An isotopically homogeneous inner terrestrial planet region. Mineral. Mag. 77, 1371.
Javoy, M., 1995. The integral enstatite chondrite model of the Earth. Geophys. Res. Lett. 22, 2219–2222.
Javoy, M., Pineau, F., 1983. Stable isotope constraints on a model Earth, from a study of mantle nitrogen. Meteoritics 18, 320–321.
Javoy, M., Kaminski, E., Guyot, F., Andrault, D., Sanloup, C., Moreira, M., Labrosse, S., Jambon, A., Agrinier, P., Davaille, A., 2010. The chemical composition of the Earth: enstatite chondrite models. Earth Planet. Sci. Lett. 293, 259–268.

Johansen, A., Lambrechts, M., 2017. Forming planets via pebble accretion. Annu. Rev. Earth Planet. Sci. 45, 359–387.
Jordan, M.K., Young, E.D., Jacobsen, S.B., 2013. Mg and Si isotope fractionation in Allende CAI SJ101 as a result of condensation. Lunar Planet. Sci. 44. #3052.
Jungck, M.H.A., Shimamura, T., Lugmair, G.W., 1984. Ca isotope variation in Allende. Geochim. Cosmochim. Acta 48, 2651–2658.
Kang, J.-T., Ionov, D.A., Liu, F., Zhang, C.-L., Golovin, A.V., Qin, L.-P., Huang, F., 2017. Calcium isotopic fractionation in mantle peridotites by melting and metasomatism and Ca isotope composition of the Bulk Silicate Earth. Earth Planet Sci. Lett. 474, 128–137.
Kargel, J.S., Lewis, J.S., 1993. The composition and early evolution of Earth. Icarus 105, 1–25.
Kleine, T., Mezger, K., Palme, H., Scherer, E., Münker, C., 2005. Early core formation in as-teroids and late accretion of chondrite parent bodies: evidence from ^{182}Hf–^{182}W in CAIs, metal-rich chondrites, and iron meteorites. Geochim. Cosmochim. Acta 69, 5805–5818.
Knight, K.B., Kita, N.T., Mendybaev, R.A., Richter, F.M., Davis, A.M., Valley, J.W., 2009. Silicon isotopic fractionation of CAI- like vacuum evaporation residues. Geochim. Cosmochim. Acta 73, 6390–6401.
Kojima, T., Tomeoka, K., 1996. Indicators of aqueous alteration and thermal metamorphism on the CV parent body: Microtextures of a dark inclusion from Allende. Geochim. Cosmochim. Acta 60, 2651–2666.
Kööp, L., Davis, A.M., Nakashima, D., Park, C., Krot, A.N., Nagashima, K., Tenner, T.J., Heck, P.R., Kita, N.T., 2016a. A link between oxygen, calcium and titanium isotopes in ^{26}Al-poor hibonite-rich CAIs from Murchison and implications for the heterogeneity of dust reservoirs in the Solar nebula. Geochim. Cosmochim. Acta 189, 70–95.
Kööp, L., Nakashima, D., Heck, P.R., Kita, N.T., Tenner, T.J., Krot, A.N., Nagashima, K., Park, C., Davis, A.M., 2016b. New constraints on the relationship between ^{26}Al and oxygen, calcium, and titanium isotopic variation in the early Solar System from a multielement isotopic study of spinel-hibonite inclusions. Geochim. Cosmochim. Acta 184, 151–172.
Kööp, L., Davis, A.M., Krot, A.N., Nagashima, K., Simon, S.B., 2018a. Calcium and titanium isotopes in refractory inclusions from CM, CO, and CR chondrites. Earth Planet. Sci. Lett. 489, 179–190.
Kööp, L., Nakashima, D., Heck, P.R., Kita, N.T., Tenner, T.J., Krot, A.N., Nagashima, K., Park, C., Davis, A.M., 2018b. A multielement isotopic study of refractory FUN and CAIs: mass-dependent and mass-independent isotope effects. Geochim. Cosmochim. Acta 221, 296–317.
Krot, A.N., Meibom, A., Keil, K., 2000a. A clast of Bali-like oxidized CV material in the reduced CV chondrite breccia Vigarano. Meteorit. Planet. Sci. 35, 817–825.
Krot, A.N., Petaev, M.I., Meibom, A., Keil, K., 2000b. In situ growth of Ca-rich rims around Allende dark inclusions. Geochim. Int. 38, S351–S368.
Krot, A.N., Makide, K., Nagashima, K., Huss, G.R., Ogliore, R.C., Ciesla, F.J., Yang, L., Hellebrand, E., Gaidos, E., 2012. Heterogeneous distribution of ^{26}Al at the birth of the Solar System: evidence from refractory grains and inclusions. Meteorit. Planet. Sci. 47, 1948–1979.
Krot, A.N., Keil, K., Scott, E.R.D., Goodrich, C.A., Weisberg, M.K., 2014. Classification of meteorites and their genetic relationships. In: Davis, A.M. (Ed.), Meteorites and Cosmochemical Processes. Elsevier, Oxford, pp. 1–63. Vol. 1 Treatise on Geochemistry, 2nd Ed. (Exec. Eds. Holland, H. D., and Turekian, K. K.).
Kruijer, T.S., Touboul, M., Fischer-Godde, M., Bermingham, K.R., Walker, R.J., Kleine, T., 2014. Protracted core formation and rapid accretion of protoplanets. Science 344, 1150–1154.
Kurat, G., Palme, H., Brandstatter, F., Huth, J., 1989. Allende xenolith AF: undisturbed record of condensation and aggregation of matter in the Solar nebula. Z. Naturforsch. A 10, 988–1004.
Larimer, J.W., 1971. Composition of the Earth: chondritic or achondritic? Geochim. Cosmochim. Acta 35, 769–786.
Larsen, K.K., Trinquier, A., Paton, C., Schiller, M., Wielandt, D., Ivanova, M.A., Connelly, J.N., Nordlund, Å., Krot, A.N., Bizzarro, M., 2011. Evidence for magnesium isotope heterogeneity in the Solar protoplanetary disk. Astrophys. J. 735, L37–L47.
Lee, T., Papanastassiou, D.A., Wasserburg, G.J., 1978. Calcium isotopic anomalies in the Allende Meteorite. Astrophys. J. 220, L21–L25.
Lee, T., Russell, W.A., Wasserburg, G.J., 1979. Calcium isotopic anomalies and the lack of aluminum-26 in an unusual Allende inclusion. Astrophys. J. 228, L93–L98.
Lee, T., Mayeda, T.K., Clayton, R.N., 1980. Oxygen isotopic anomalies in Allende inclusion HAL. Geophys. Res. Lett. 7, 493–496.
Lewis, R.S., Srinivasan, B., Anders, E., 1975. Host phase of a strange xenon component in Allende. Science 190, 1251–1262.
Lewis, R.S., Tang, M., Wacker, J.F., Anders, E., Steel, E., 1987. Interstellar diamonds in meteorites. Nature 326, 160–162.
Liebske, C., Khan, A., 2019. On the principal building blocks of Mars and Earth. Icarus 322, 121–134.
Liu, M.-C., 2017. The Initial ^{41}Ca/^{40}Ca Ratios in Two Type A ca-Al-Rich Inclusions: Implications Fort he Origin of Short-Lived ^{41}Ca.
Liu, M.-C., McKeegan, K., Goswami, J.N., Marhas, K.K., Sahijpal, S., Ireland, T.R., Davis, A.M., 2009. Isotopic records in CM hibonites: implications for timescales of mixing of isotope reservoirs in the Solar nebula. Geochim. Cosmochim. Acta 73, 5051–5079.
Liu, M.-C., Chaussidon, M., Srinivasan, G., McKeegan, K., 2012. A lower initial abundance of short-lived ^{41}Ca in the early Solar System and its implications for Solar System formation. Astrophys. J. 761, 137.
Liu, M.-C., Han, J., Brearley, A.J., Hertwig, A.T., 2019. Aluminum-26 chronology of dust coagulation and early Solar System evolution. Sci. Adv. 5 eaaw3350.
Lock, S.J., Stewart, S.T., Petaev, M.I., Leinhardt, Z., Mace, M.T., Jacobsen, S.B., Ćuk, M., 2018. The origin of the Moon with a terrestrial synestia. J. Geophys. Res.: Planets 123, 910–951.
Lock, S.J., Bermingham, K.R., Parai, R., Boyet, M., 2020. Geochemical constraints on the origin of the Moon and preservation of ancient terrestrial heterogeneities. Space Sci. Rev. 216, 109.
Lodders, K., 2003. Solar system abundances and condensation temperatures of the elements. Astrophys. J. 591, 1220–1247.
Lodders, K., 2020. Solar Elemental Abundances, in the Oxford Research Encyclopedia of Planetary Science. Oxford University Press.
Lodders, K., Amari, S., 2005. Grains from meteorites: remnants from the early times of the Solar System. Chem. Erde 65, 93–166.
Lodders, K., Fegley, B., 1997. An oxygen isotope model for the composition of Mars. Icarus 126, 373–394.
Lugmair, G.W., Shukolyukov, A., 1998. Early Solar System timescales according to ^{53}Mn-^{53}Cr systematics. Geochim. Cosmochim. Acta 62, 2863–2886.
Lundberg, L.L., Zinner, E., Crozaz, G., 1994. Search for isotopic anomalies in oldhamite (CaS) from unequilibrated (E3) enstatite chondrites. Meteorit. Planet. Sci. 29, 384–393.
MacPherson, G.J., 2014. Calcium-aluminum-rich inclusions in chondritic meteorites. In: Davis, A.M. (Ed.), Meteorites and Cosmochemical Processes. Elsevier, Oxford, pp. 139–179. Vol. 1 Treatise on Geochemistry, 2nd Ed. (Exec. Eds. Holland, H. D. and Turekian, K. K.).
MacPherson, G.J., Bar-Matthews, M., Tanaka, T., Olsen, E., Grossman, L., 1983. Refractory inclusions in the Murchison meteorite. Geochim. Cosmochim. Acta 47, 823–839.
MacPherson, G.J., Davis, A.M., Zinner, E., 1995. The distribution of aluminum-26 in the early Solar System – a reappraisal. Meteoritics 30, 365–368.
MacPherson, G.J., Simon, S.B., Davis, A.M., Grossman, L., Krot, A.N., 2005. Calcium-aluminum-rich inclusions: Major unanswered questions. In: Krot, A.N., Scott, E.R.D., Reipurth, B. (Eds.), Chondrites and the Protoplanetary Disk, Astronomical Society of the Pacific Conference Series, vol. 341.
MacPherson, G.J., Kita, N.T., Ushikubo, T., Bullock, E.S., Davis, A.M., 2012. Well-resolved variations in the formation ages for Ca–Al-rich inclusions in the early Solar System. Earth Planet. Sci. Lett. 331-332, 43–54.
Magna, T., Gussone, N., Mezger, K., 2015. The calcium isotope systematics of Mars. Earth Planet. Sci. Lett. 430, 86–94.
Martin, P.M., Mason, B., 1974. Major and trace elements in the Allende meteorite. Nature 249, 333–334.
Mason, B., Taylor, S.R., 1982. Inclusions in the Allende meteorite. Smithson. Contrib. Earth Sci. 25, 1–30.
McDonough, W.F., Sun, S.-S., 1995. The composition of the Earth. Chem. Geol. 120, 223–253.
McGuire, A.V., Hashimoto, A., 1989. Origin of zoned fine-grained inclusions in the Allende meteorite. Geochim. Cosmochim. Acta 53, 1123–1133.
McSween Jr., H.Y., 1987. Aqueous alteration in carbonaceous chondrites: mass balance constraints on matrix mineralogy. Geochim. Cosmochim. Acta 51, 2469–2477.
Mendybaev, R.A., Beckett, J.R., Grossman, L., Stolper, E., Cooper, R.F., Bradley, J.P., 2002. Volatilization kinetics of silicon carbide in reducing gases: an experimental study with applications to the survival of presolar grains in the Solar nebula. Geochim. Cosmochim. Acta 66, 661–682.
Meyer, B.S., Krishnan, T.D., Clayton, D.D., 1996. ^{48}Ca production in matter expanding from high temperature and density. Astrophys. J. 462, 825.
Mittlefehldt, D.W., 2014. Achondrites. In: Davis, A.M. (Ed.), Meteorites and Cosmochemical Processes. Elsevier, Oxford, pp. 235–266. Vol. 1 Treatise on Geochemistry, 2nd Ed. (Exec. Eds. Holland, H. D. and Turekian, K. K.).
Mohapatra, R.K., Murty, S.V.S., 2003. Precursors of Mars: constraints from nitrogen and oxygen isotopic compositions of Martian meteorites. Meteorit. Planet. Sci. 38, 225–241.
Montmerle, T., Augereau, J.-C., Chaussidon, M., Gounelle, M., Marty, B., Morbidelli, A., 2006. Solar system formation and early evolution: the first 100 million years. Earth Moon Planet. 98, 39–95.
Mougel, B., Moynier, F., Gopel, C., 2017. Chromium isotopic homogeneity between the Moon, the Earth, and enstatite chondrites. Earth Planet. Sci. Lett. 481, 1–8.
Moynier, F., Simon, J.I., Podosek, F.I., Meyer, B.S., Brannon, J., DePaolo, D.J., 2010. Ca isotope effects in Orgueil leachates and the implications for the carrier phases of ^{54}Cr anomalies. Astrophys. J. 718, L7–L13.
Moynier, F., Day, J.M.D., Okui, W., Yokoyama, T., Bouvier, A., Walker, R.J., Podosek, F. A., 2012. Planetary-scale strontium isotopic heterogeneity and the age of volatile depletion of early Solar System materials. Astrophys. J. 758, 45.
Nagahara, H., Ozawa, K., 2000. The role of back reaction on chemical fractionation during evaporation of a condensed phase. Lunar Planet. Sci. 31. #1340.
Niederer, F.R., Papanastassiou, D.A., 1979. Ca isotopes in Allende and Leoville inclusions. Lunar Planet. Sci. 10, 913–915.
Niederer, F.R., Papanastassiou, D.A., 1984. Ca isotopes in refractory inclusions. Geochim. Cosmochim. Acta 48, 1279–1293.
Nishiizumi, K., Fink, D., Klein, J., Middleton, R., Masarik, J., Reedy, R.C., Arnold, J.R., 1997. Depth profile of ^{41}Ca in an Apollo 15 drill core and the low-energy neutron flux in the Moon. Earth Planet. Sci. Lett. 148, 545–552.
Nittler, L.R., McCoy, T.J., Clark, P.E., Murphy, M.E., Trombka, J.I., Jarosewich, E., 2004. Bulk element compositions of meteorites: a guide for interpreting remote-sensing geochemical measurements of planets and asteroids. Antarctic Meteorite Res. 17, 231.
O'Brien, D.P., Morbidelli, A., Levison, H.F., 2006. Terrestrial planet formation with strong dynamical friction. Icarus 18, 39–58.

Pahlevan, K., Stevenson, D.J., 2007. Equilibration in the aftermath of the lunar-forming giant impact. Earth Planet. Sci. Lett. 262, 438–449.
Palme, H., O'Neill, H., 2014. Cosmochemical estimates of mantle composition. In: Carlson, R.W. (Ed.), The Mantle and Core. Elsevier, Oxford, pp. 1–39. Vol. 3 Treatise on Geochemistry, 2nd Ed. (Exec. Eds. Holland, H. D. and Turekian, K. K.).
Palme, H., Lodders, K., Jones, A., 2014. Solar System abundances of the elements. In: Davis, A.M. (Ed.), Planets, Asteroids, Comets, and the Solar System. Elsevier, Oxford, pp. 15–36. Vol. 2 Treatise on Geochemistry, 2nd Ed. (Exec. Eds. Holland, H. D. and Turekian, K. K.).
Pape, J., Mezger, K., Bouvier, A., Baumgartner, L.P., 2019. Time and duration of chondrule formation: constraints from ^{26}Al-^{26}Mg ages of individual chondrules. Geochim. Cosmochim. Acta 244, 416–436.
Park, C., Nagashima, K., Wasserburg, G.J., Papanastassiou, D.A., Hutcheon, I.D., Davis, A.M., Huss, G.R., Bizzarro, M., Krot, A.N., 2014. Calcium and titanium isotopic compositions of FUN CAIs: implications for their origin. Lunar Planet. Sci. 45. #2656.
Park, C., Nagashima, K., Krot, A.N., Huss, G.R., Davis, A.M., Bizzarro, M., 2017. Calcium-aluminum-rich inclusions with fractionation and unidentified nuclear effects (FUN CAIs): II. Heterogeneities of magnesium isotopes and ^{26}Al in the early Solar System inferred from in situ high-precision magnesium-isotope measurements. Geochim. Cosmochim. Acta 201, 6–24.
Petaev, M.I., Jacobsen, S.B., 2009. Petrologic study of SJ101, a new forsterite-bearing CAI from the Allende CV3 chondrite. Geochim. Cosmochim. Acta 73, 5100–5114.
Petaev, M.I., Wood, J.A., 1998. The condensation with partial isolation (CWPI) model of condensation in the Solar nebula. Meteorit. Planet. Sci. 33, 1123–1137.
Poitrasson, F., Halliday, A.N., Lee, D.-C., Levasseur, S., Teutsch, N., 2004. Fe isotope differences between Earth, Moon, Mars and Vesta as possible records of contrasted accretion mechanisms. Earth Planet. Sci. Lett. 223, 253–266.
Qin, L., Carlson, R.W., 2016. Nucleosynthetic isotope anomalies and their cosmochemical significance. Geochem. J. 50, 43–65.
Qin, L., Alexander, C.M.O., Carlson, R.W., Horan, M.F., Yokoyama, T., 2010. Contributors to chromium isotope variation of meteorites. Geochim. Cosmochim. Acta 74, 1122–1145.
Raymond, S.N., O'Brien, D.P., Morbidelli, A., Kaib, N.A., 2009. Building the terrestrial planets: constrained accretion in the inner Solar System. Icarus 203, 644–662.
Regelous, M., Elliott, T., Coath, C.D., 2008. Nickel isotope heterogeneity in the early Solar System. Earth Planet. Sci. Lett. 272, 330–338.
Reynolds, J.H., Turner, G., 1964. Rare gases in the chondrite Renazzo. J. Geophys. Res. 69, 3263–3281.
Richter, F.M., Davis, A.M., Ebel, D.S., Hashimoto, A., 2002. Elemental and isotopic fractionation of Type B calcium-, aluminum-rich inclusions: experiments, theoretical considerations, and constraints on their thermal evolution. Geochim. Cosmochim. Acta 66, 521–540.
Richter, F.M., Janney, P.E., Mendybaev, R.A., Davis, A.M., Wadhwa, M., 2007. Elemental and isotopic fractionation of Type B CAI-like liquids by evaporation. Geochim. Cosmochim. Acta 71, 5544–5564.
Rubie, D.C., Jacobson, S.A., Morbidelli, A., O'Brien, D.P., Young, E.D., de Vries, J., Nimmo, F., Palme, H., Frost, D.J., 2015. Accretion and differentiation of the terrestrial planets with implications for the compositions of early-formed Solar System bodies and accretion of water. Icarus 248, 89–108.
Rubin, A.E., Wasson, J.T., 1995. Variations of chondrite properties with heliocentric distance. Meteoritics 30, 569.
Russell, W.A., Papanastassiou, D.A., Tombrello, T.A., 1978. Calcium isotope fractionation on the Earth and other Solar System materials. Geochim. Cosmochim. Acta 42, 1075–1090.
Russell, S.S., Huss, G.R., Fahey, A.J., Greenwood, R.C., Hutchison, R., Wasserburg, G.J., 1998. An isotopic and petrologic study of calcium-aluminum-rich inclusions from CO3 meteorites. Geochim. Cosmochim. Acta 62, 689–714.
Ruzicka, A., Floss, C., Hutson, M., 2012. Amoeboid olivine aggregates (AOAs) in the Efremovka, Leoville and Vigarano (CV3) chondrites: A record of condensate evolution in the Solar nebula. Geochim. Cosmochim. Acta 79, 79–105.
Sahijpal, S., Goswami, J.N., Davis, A.M., Grossman, L., Lewis, R.S., 1998. A stellar origin for the short-lived nuclides in the early Solar System. Nature 391, 559–561.
Sahijpal, S., Goswami, J.N., Davis, A.M., 2000. K, Mg, Ti and Ca isotopic compositions and refractory trace element abundances in hibonites from CM and CV meteorites: Implications for early Solar System processes. Geochim. Cosmochim. Acta 64, 1989–2005.
Sanloup, C., Jambon, A., Gillet, P., 1999. A simple chondritic model of Mars. Phys. Earth Planet. Inter. 112, 43–54.
Savage, P.S., Moynier, F., 2013. Si isotopic variations in enstatite meteorites: clues to their origin. Earth Planet. Sci. Lett. 361, 487–496.
Schiller, M., Paton, C., Bizzarro, M., 2015. Evidence for nucleosynthetic enrichment of the protoSolar molecular cloud core by multiple supernova events. Geochim. Cosmochim. Acta 149, 88–102.
Schiller, M., Bizzarro, M., Fernandes, V.A., 2018. Isotopic evolution of the protoplanetary disk and the building blocks of Earth and the Moon. Nature 555, 507–510.
Schönbächler, M., Carlson, R.W., Horan, M.F., Mock, T.D., Hauri, E.H., 2010. Heterogeneous accretion and the moderately volatile element budget of Earth. Science 328, 884–887.
Scott, E.R.D., Krot, A.N., 2014. Chondrites and their components. In: Davis, A.M. (Ed.), Meteorites and Cosmochemical Processes. Elsevier, Oxford, pp. 65–137. Vol. 1 Treatise on Geochemistry, 2nd Ed. (Exec. Eds. Holland, H. D. and Turekian, K. K.).
Sedaghatpour, F., Teng, F.-Z., Liu, Y., Sears, D.W.G., Taylor, L.A., 2013. Magnesium isotopic composition of the Moon. Geochim. Cosmochim. Acta 120, 1–16.
Shahar, A., Young, E.D., 2007. Astrophysics of CAI formation as revealed by silicon isotope LA-MC-ICPMS of an igneous CAI. Earth Planet. Sci. Lett. 257, 497–510.
Shu, F.H., Adams, F.C., Lizano, S., 1987. Star formation in molecular clouds: Observation and theory. Annu. Rev. Astron. Astrophys. 25, 23–72.
Simon, J.I., DePaolo, D.J., 2010. Stable calcium isotopic composition of meteorites and rocky planets. Earth Planet. Sci. Lett. 289, 457–466.
Simon, J.I., Young, E.D., 2011. Resetting, errorchrons and the meaning of canonical CAI initial ^{26}Al/^{27}Al values. Earth Planet. Sci. Lett. 304, 468–482.
Simon, J.I., Young, E.D., Russell, S.S., Tonui, E.K., Dyl, K.A., Manning, C.E., 2005. A short timescale for changing oxygen fugacity in the Solar nebula revealed by high-resolution ^{26}Al- ^{26}Mg dating of CAI rims. Earth Planet. Sci. Lett. 238, 272–283.
Simon, J.I., DePaolo, D.J., Moynier, F., 2009. Calcium isotopic composition of meteorites, Earth, and Mars. Astrophys. J. 702, 707–715.
Simon, J.I., Jordan, M.K., Tappa, M.J., Schauble, E.A., Kohl, I.E., Young, E.D., 2017. Calcium and titanium isotope fractionation in refractory inclusions: tracers of condensation and inheritance in the early Solar protoplanetary disk. Earth Planet. Sci. Lett. 472, 277–288.
Simon, J.I., Cuzzi, J.N., McCain, K., Christoffersen, P., Srinivasan, P., Fisher, K., Tait, A. W., Olson, J.N., Scargle, J., 2018. Particle size distributions in chondritic meteorites: evidence for pre-planetesimal histories. Earth Planet. Sci. Lett. 494, 69–82.
Simon, J.I., Ross, D.K., Nguyen, A.N., Simon, S.B., Messenger, S., 2019. Molecular cloud origin for oxygen isotopic heterogeneity recorded by a primordial spinel-rich refractory inclusion. Astrophys. J. Lett. 884. #L29 (9 pp).
Skulan, J., DePaolo, D.J., Owens, T.L., 1997. Biological control of calcium isotopic abundances in the global calcium cycle. Geochim. Cosmochim. Acta 61, 2505–2510.
Spicuzza, M.J., Day, J.M.D., Taylor, L.A., Valley, J.W., 2007. Oxygen isotope constraints on the origin and differentiation of the Moon. Earth Planet. Sci. Lett. 253, 254–265.
Srinivasan, G., Ulyanov, A.A., Goswami, J.N., 1994. ^{41}Ca in the early Solar System. Astrophys. J. 431, L67–L70.
Srinivasan, G., Sahijpal, S., Ulyanov, A.A., Goswami, J.N., 1996. Ion microprobe studies of Efremovka CAIs: II. Potassium isotope composition and ^{41}Ca in the early Solar System. Geochim. Cosmochim. Acta 60, 1823–1835.
Tang, H., Dauphas, N., 2014. ^{60}Fe–^{60}Ni chronology of core formation on Mars. Earth Planet. Sci. Lett. 390, 264–274.
Teng, F.-Z., Li, W.-Y., Ke, S., Marty, B., Dauphas, N., Huang, S., Wu, F.-Y., Pourmand, A., 2010. Magnesium isotopic composition of the Earth and chondrites. Geochim. Cosmochim. Acta 74, 4150–4166.
Thiemens, M.H., Heidenreich, J.E., 1983. The mass-independent fractionation of oxygen: a novel isotope effect and its possible cosmochemical implications. Science 219, 1073–1075.
Torrano, Z.A., Brennecka, G.A., Williams, C.D., Romaniello, S.J., Hines, R.R., Wadhwa, M., 2019. Titanium isotope signatures of calcium-aluminum-rich inclusions from CV and CK chondrites: implications for early Solar System reservoirs and mixing. Geochim. Cosmochim. Acta 263, 13–30.
Trinquier, A., Elliott, T., Ulfbeck, D., Coath, C., Krot, A.N., Bizzarro, M., 2009. Origin of nucleosynthetic isotope heterogeneity in the Solar protoplanetary disk. Science 324, 374–376.
Valdes, M.C., Moreira, M., Foriel, J., Moynier, F., 2014. The nature of Earth's building blocks as revealed by calcium isotopes. Earth Planet. Sci. Lett. 394, 135–145.
Valdes, M.C., Debaille, V., Berger, J., Armytage, R.M.G., 2019. The effects of high-temperature fractional crystallization on calcium isotopic composition. Chem. Geol. 509, 77–91.
Wanajo, S., Janka, H.-T., Muller, B., 2013. Electron-capture supernovae as origin of ^{48}Ca. Astrophys. J. 767. #L26 (6 pp).
Wang, K., Savage, P.S., Moynier, F., 2014. The iron isotope composition of enstatite meteorites: implications for their origin and the metal/sulfide Fe isotopic fractionation factor. Geochim. Cosmochim. Acta 142, 149–165.
Wark, D., Boynton, W.V., 2001. The formation of rims on calcium-aluminum-rich inclusions: step I-flash heating. Meteorit. Planet. Sci. 36, 1135–1166.
Warren, P.H., 2011. Stable-isotopic anomalies and the accretionary assemblage of the Earth and Mars: a subordinate role for carbonaceous chondrites. Earth Planet. Sci. Lett. 311, 93–100.
Wasserburg, G.J., Trippella, O., Busso, M., 2015. Isotope anomalies in the Fe- group elements in meteorites and connections to nucleosynthesis in AGB Stars. Astrophys. J. 805, 7.
Wasson, J.T., Kallemeyn, G.W., 1988. Compositions of chondrites. Philos. Trans. R. Soc. A 325, 535–544.
Wasson, J.T., Wetherill, G.W., 1979. Dynamical chemical and isotopic evidence regarding the formation locations of asteroids and meteorites. In: Gehrels, T. (Ed.), Asteroids. University of Arizona Press, Tucson, pp. 926–974.
Weber, D., Zinner, E.K., Bischoff, A., 1995. Trace element abundances and magnesium, calcium, and titanium isotopic compositions of grossite-containing inclusions from the carbonaceous chondrite Acfer 182. Geochim. Cosmochim. Acta 59, 803–823.
Weisberg, M.K., McCoy, T.J., Krot, A.N., 2006. Systematics and evaluation of meteorite classification. In: Lauretta, D.S., McSween Jr., H.Y. (Eds.), Meteorites and the Early Solar System II. University of Arizona Press, Tucson, pp. 19–52.
Wiechert, U., Halliday, A.N., Lee, D.-C., Snyder, G.A., Rumble, D., 2001. Oxygen isotopes and the Moon-forming giant impact. Science 294, 345–348.
Wimpenny, J.B., Yin, Q.Z., Zipfel, J., MacPherson, G., Ebel, D.S., Heck, P.R., 2014. Renewed search for FUN based on Al-Mg systematics in CAIs with LA-MC-ICP-MS. Lunar Planet. Sci. 45. #2235.
Wood, J.A., 2005. The chondrite types and their origins. In: Krot, A.N., Scott, E.R.D., Reipurth, B. (Eds.), Chondrites and the Protoplanetary Disk, ASP Conference Series, pp. 953–971.
Yamada, M., Tachibana, S., Nagahara, H., Ozawa, K., 2006. Anisotropy of Mg isotopic fractionation during evaporation and Mg self-diffusion of forsterite in vacuum. Planet. Space Sci. 54, 1096–1106.

Yin, Q.-Z., Yamashita, K., Yamakawa, A., Tanaka, R., Jacobsen, B., Ebel, D.S., Hutcheon, I.D., Nakamura, E., 2009. ^{53}Mn-^{53}Cr systematics of Allende chondrules and epsilon ^{54}Cr–Δ^{17}O correlation in bulk carbonaceous chondrites. Lunar Planet. Sci. 40. #2006.

Yokoyama, T., Misawa, K., Okano, O., Shih, C.-Y., Nyquist, L.E., Simon, J.I., Tappa, M.J., Yoneda, S., 2017. Extreme early Solar System chemical fractionation recorded by alkali-rich clasts contained in ordinary chondrite breccias. Earth Planet. Sci. Lett. 458, 233–240.

Yoneda, S., Grossman, L., 1995. Condensation of CaO-MgO-Al_2O_3-SiO_2 liquids from cosmic gases. Geochim. Cosmochim. Acta 59, 3413–3444.

Young, E.D., Nagahara, H., Mysen, B.O., Audet, D.M., 1998. Non-rayleigh oxygen isotope fractionation by mineral evaporation: Theory and experiments in the system SiO_2. Geochim. Cosmochim. Acta 62, 3109–3116.

Young, E.D., Galy, A., Nagahara, H., 2002. Kinetic and equilibrium mass-dependent isotope fractionation laws in nature and their geochemical and cosmochemical significance. Geochim. Cosmochim. Acta 66, 1095–1104.

Young, E.D., Kohl, I.E., Warren, P.H., Rubie, D.C., Jacobson, S.A., Morbidelli, A., 2016. Oxygen isotopic evidence for vigorous mixing during the Moon-forming giant impact. Science 351, 493–496.

Zhang, J., Dauphas, N., Davis, A.M., Leya, I., Fedkin, A., 2012. The proto-Earth as a significant source of lunar material. Nat. Geosci. 5, 251–255.

Zhang, J., Huang, S., Davis, A.M., Dauphas, N., Hashimoto, A., Jacobsen, S.B., 2014. Calcium and titanium isotopic fractionations during evaporation. Geochim. Cosmochim. Acta 140, 365–380.

Zinner, E., 2014. PreSolar grains. In: Davis, A.M. (Ed.), Meteorites and Cosmochemical Processes. Elsevier, Oxford, pp. 181–213. Vol. 1 Treatise on Geochemistry, 2nd Ed. (Exec. Eds. Holland, H. D. and Turekian, K. K.).

Zinner, E., Fahey, A.J., McKeegan, K.D., Goswami, J.N., Ireland, T.R., 1986. Large ^{48}Ca anomalies are associated with ^{50}Ti anomalies in Murchison and Murray hibonites. Astrophys. J. 311, L103–L107.

Zinner, E., Tang, M., Anders, E., 1987. Large isotopic anomalies of Si, C, N, and noble gases in interstellar silicon carbide from the Murray meteorite. Nature 330, 730–732.

Zolensky, M.E., McSween, H.Y., 1988. Aqueous alteration. In: Kerridge, J.F., Matthews, M.S. (Eds.), Meteorites and the Early Solar System. University of Arizona Press, pp. 114–143.